Thermal Hall effect in $SrCu_2(BO_3)_2$

Judit Romhányi

R. Ganesh

Karlo Penc

Wigner Research Centre
for Physics
Institute for Solid State
Physics and Optics
Budapest

Leibniz Institute
for Solid State and
Materials Research
Dresden

Nat. Comm. 6, 6805 (2015)
[arXiv:1406.1163]

supported by Hungarian OTKA

The Shastry-Sutherland model

exact eigenstate of a triangle:

$$\mathcal{H}_\triangle = \mathbf{S}_1 \cdot \mathbf{S}_2 + \mathbf{S}_2 \cdot \mathbf{S}_3 + \mathbf{S}_1 \cdot \mathbf{S}_3$$
$$= \frac{1}{2}\left(\mathbf{S}_1 + \mathbf{S}_2 + \mathbf{S}_3\right)^2 - \frac{9}{8}$$

$$\frac{1}{2} \otimes \frac{1}{2} \otimes \frac{1}{2} = \frac{1}{2} \oplus \frac{1}{2} \oplus \frac{3}{2}$$

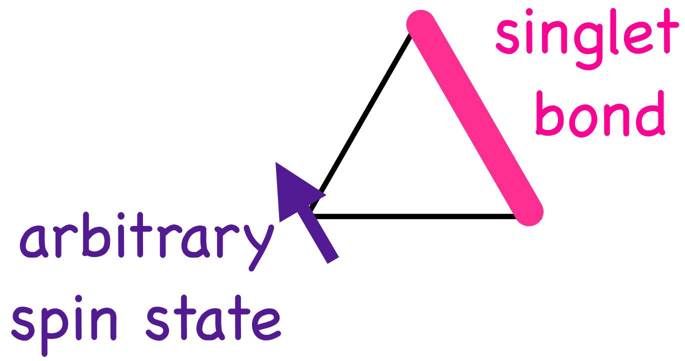

Majumdar-Ghosh model
a singlet coverings which is an exact
ground states

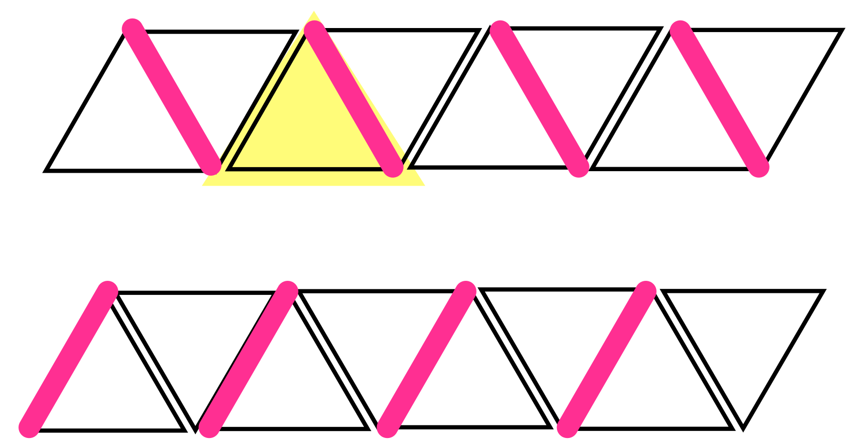

$$\mathcal{H} = \sum \mathcal{H}_\triangle = \sum_i \left(2\mathbf{S}_i \cdot \mathbf{S}_{i+1} + \mathbf{S}_i \cdot \mathbf{S}_{i+2}\right)$$

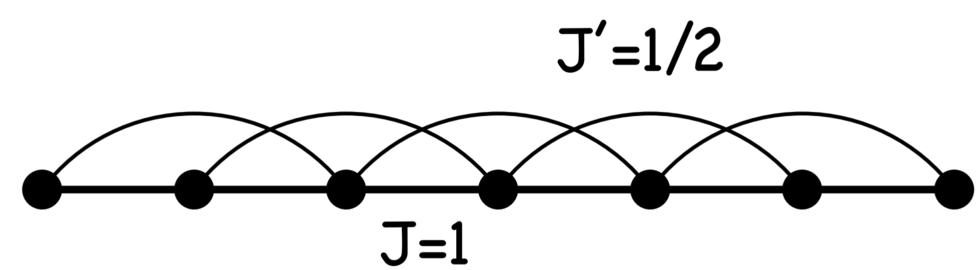

The Shastry-Sutherland model

exact eigenstate of a triangle:

$$\mathcal{H}_{\triangle} = \mathbf{S}_1 \cdot \mathbf{S}_2 + \mathbf{S}_2 \cdot \mathbf{S}_3 + \mathbf{S}_1 \cdot \mathbf{S}_3$$
$$= \frac{1}{2}\left(\mathbf{S}_1 + \mathbf{S}_2 + \mathbf{S}_3\right)^2 - \frac{9}{8}$$

$$\frac{1}{2} \otimes \frac{1}{2} \otimes \frac{1}{2} = \frac{1}{2} \oplus \frac{1}{2} \oplus \frac{3}{2}$$

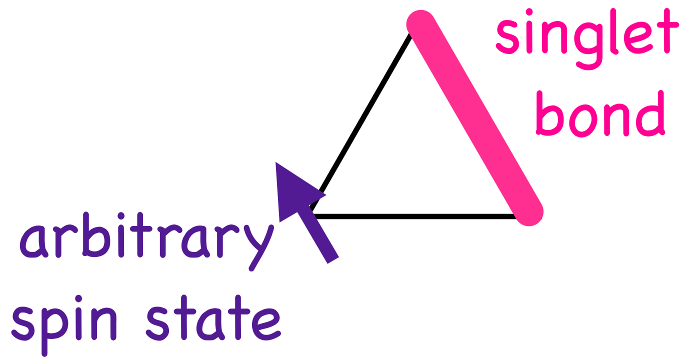

Majumdar-Ghosh model

a singlet coverings which is an exact ground states

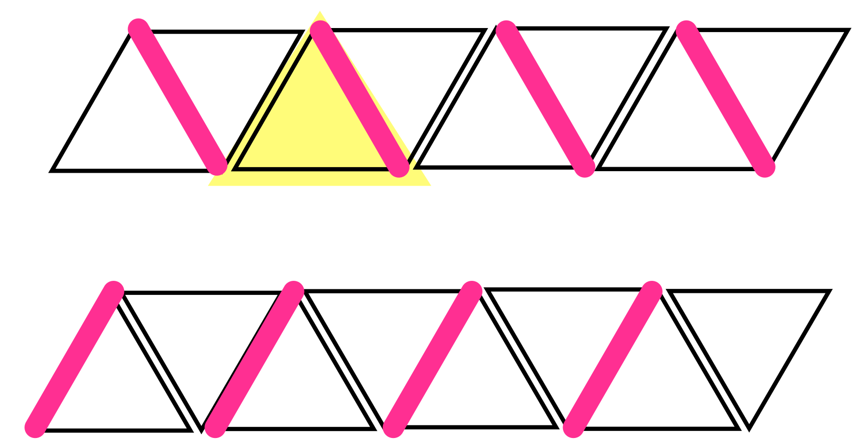

2D extension:

the dimer covering is an exact eigenstate

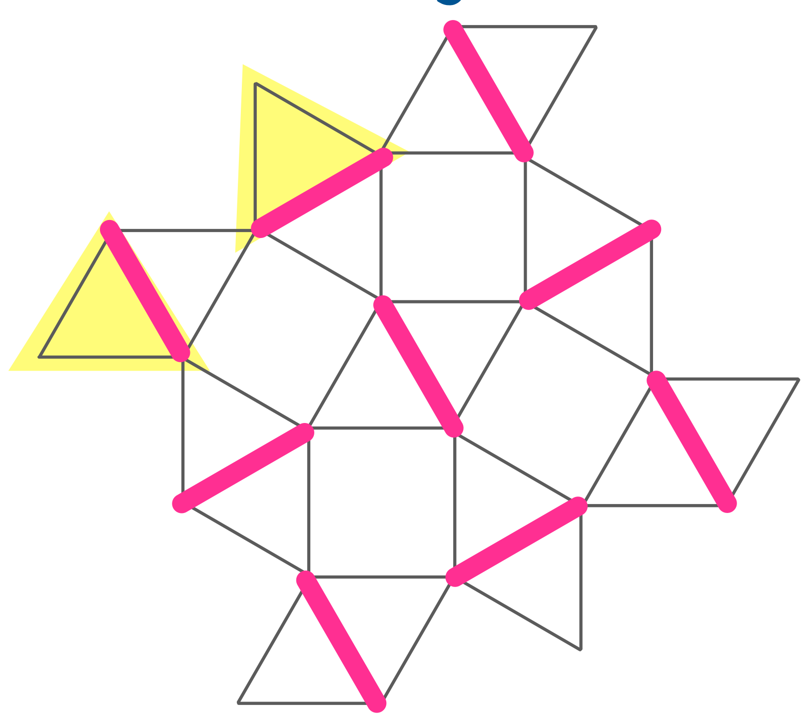

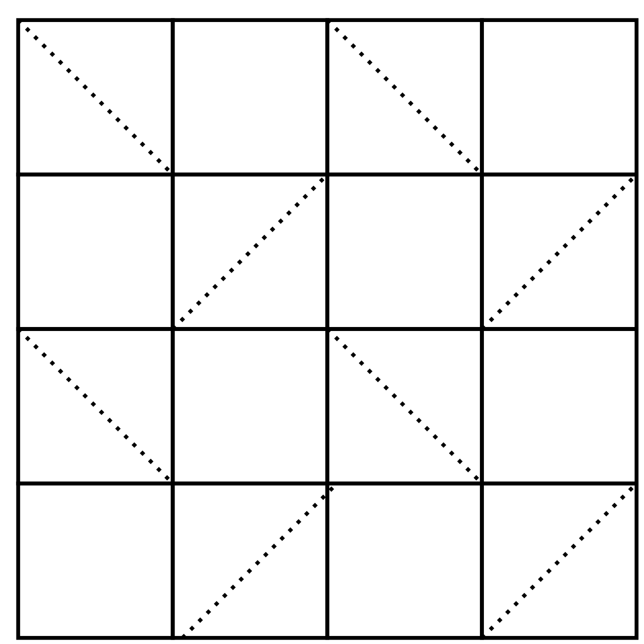

Shastry and Sutherland

Physica B **108,** 1069 (1981)

Experimental realization: $SrCu_2(BO_3)_2$

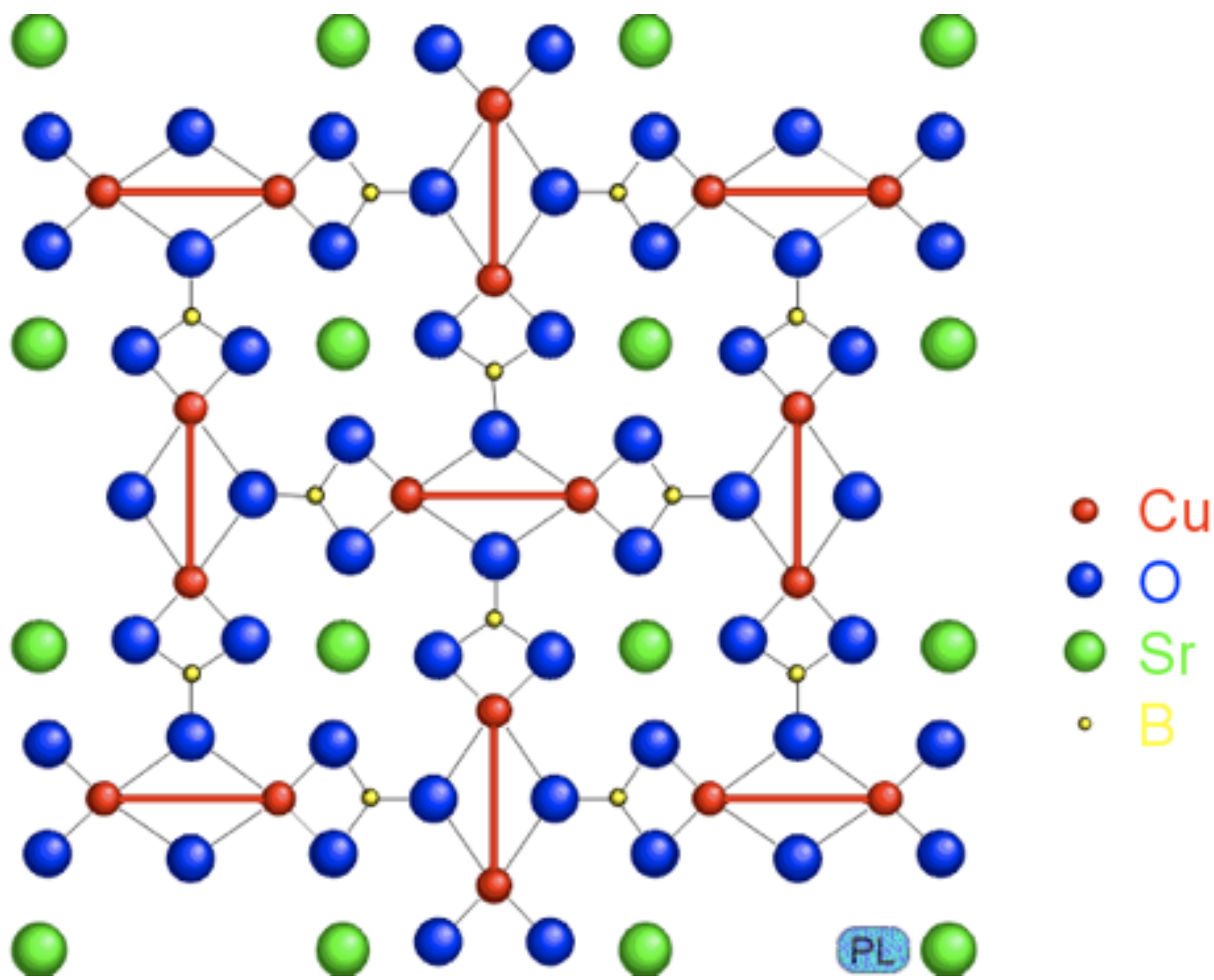

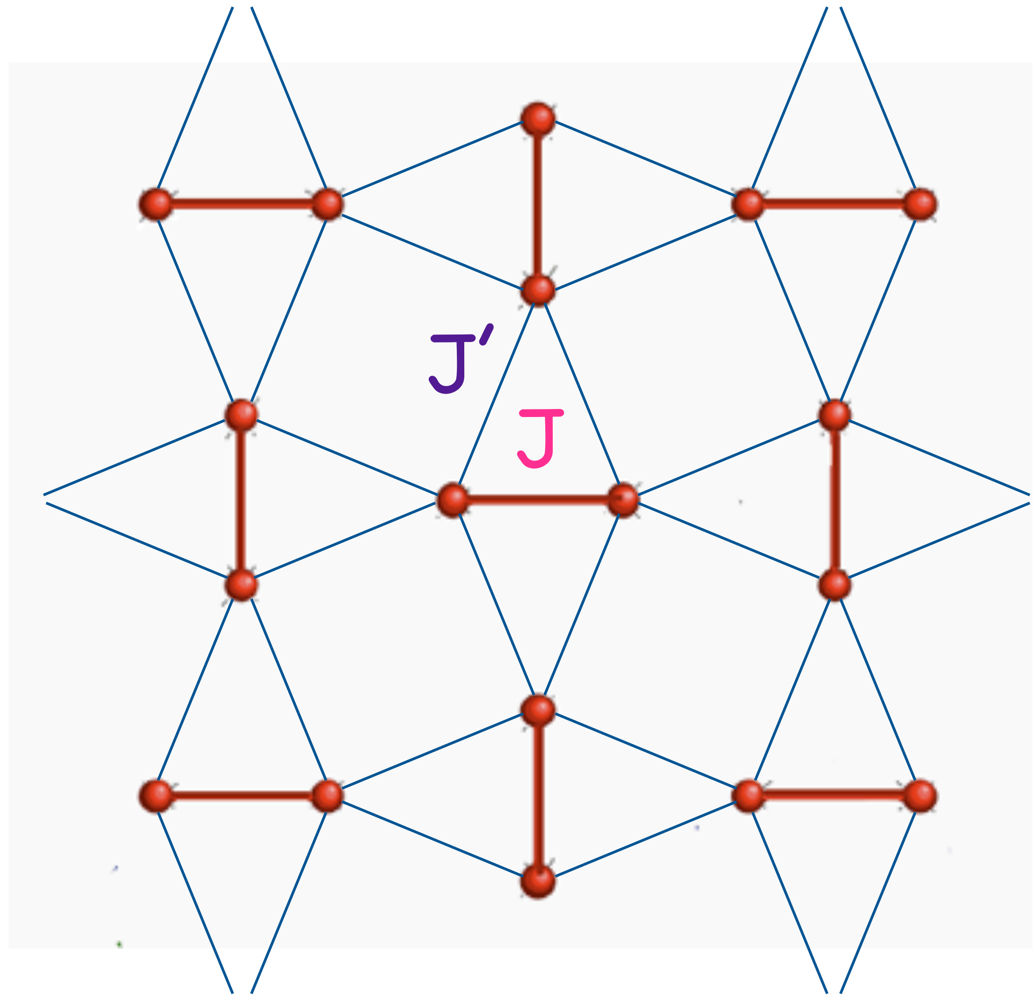

Smith & Keszler, J. Solid State Chem. **93**, 430 (1991)

Kageyama et al., Phys. Rev. Lett. **82**, 3168 (1999)

J: AFM intradimer interaction

J′: AFM interdimer interaction

Shastry-Sutherland model: singlet-dimer covering an exact ground state for $J'/J<0.7$

Magnetization

energy levels of a single dimer
in a field

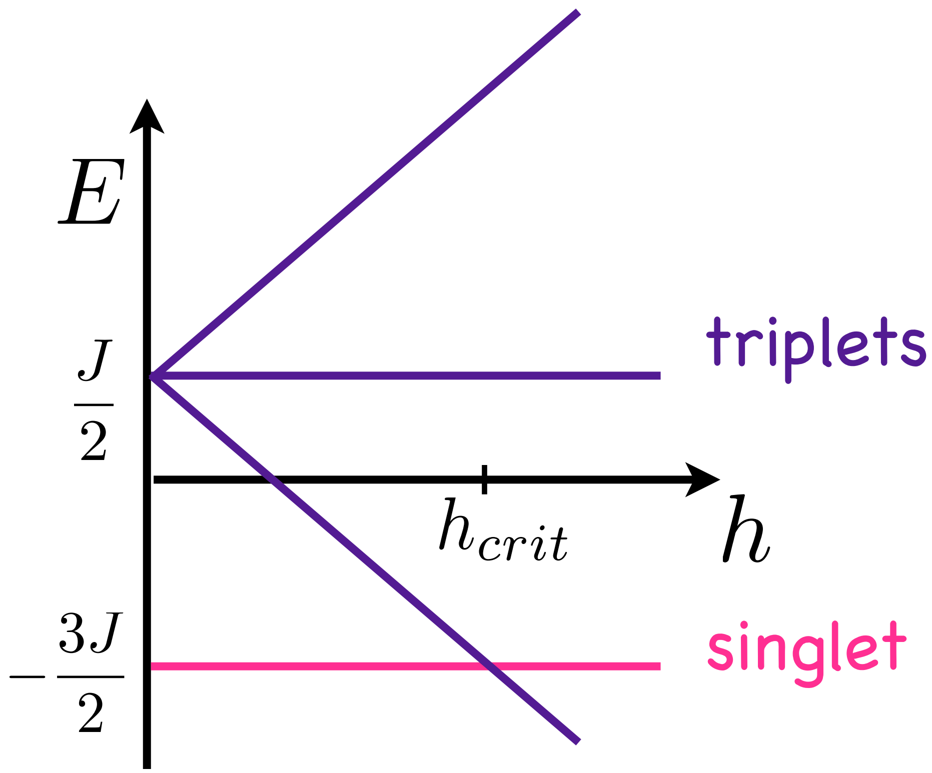

Many plateaus...

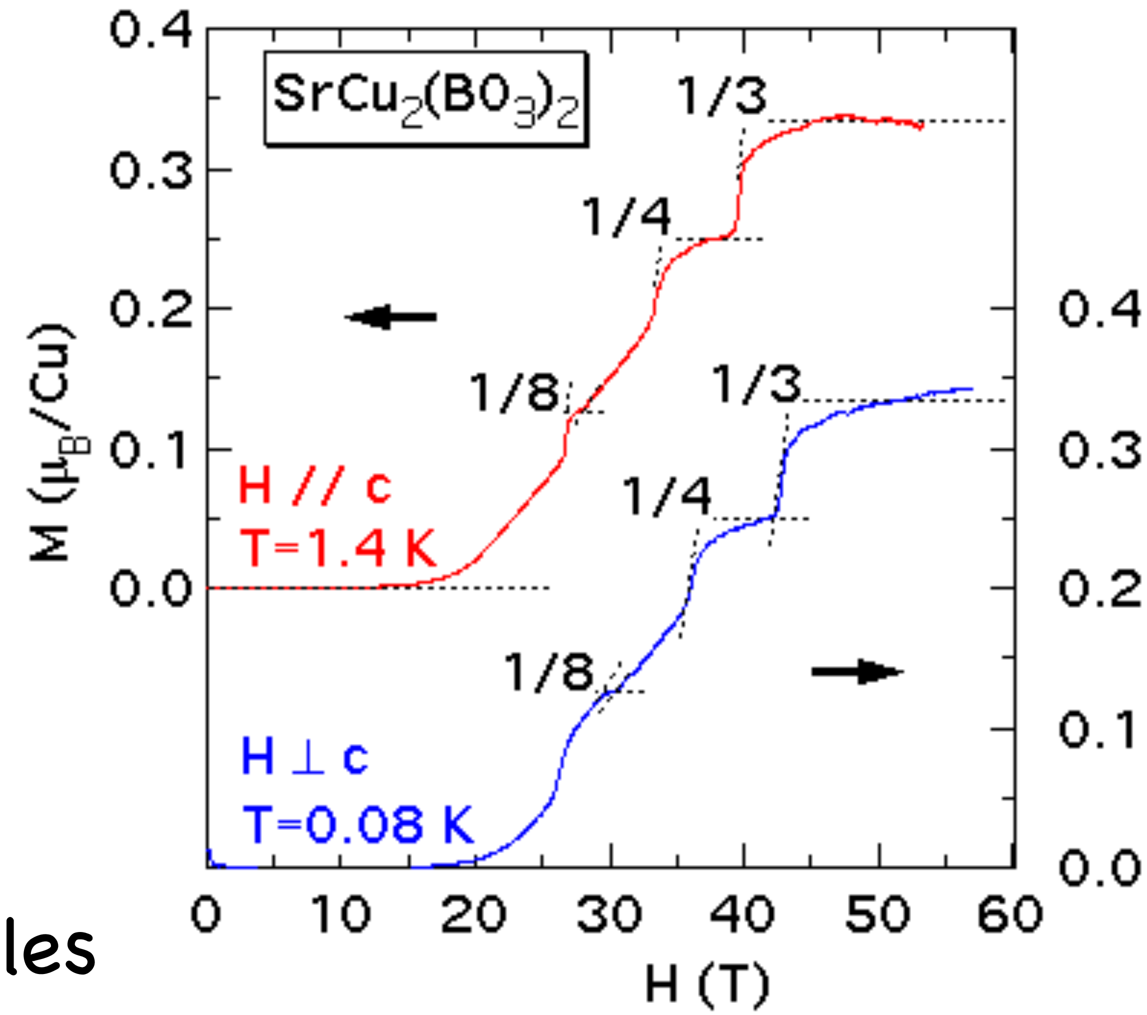

Kageyama H., et al 2002
Prog. Theor. Phys. Suppl. **145**

triplet excitations ⇨ like quasi particles on the singlet background

But in this talk we will be interested
what happens in low field...

Triplon dispersion from neutron spectra

Kageyama et al., Phys. Rev. Lett. **84**, 5876 (2000)

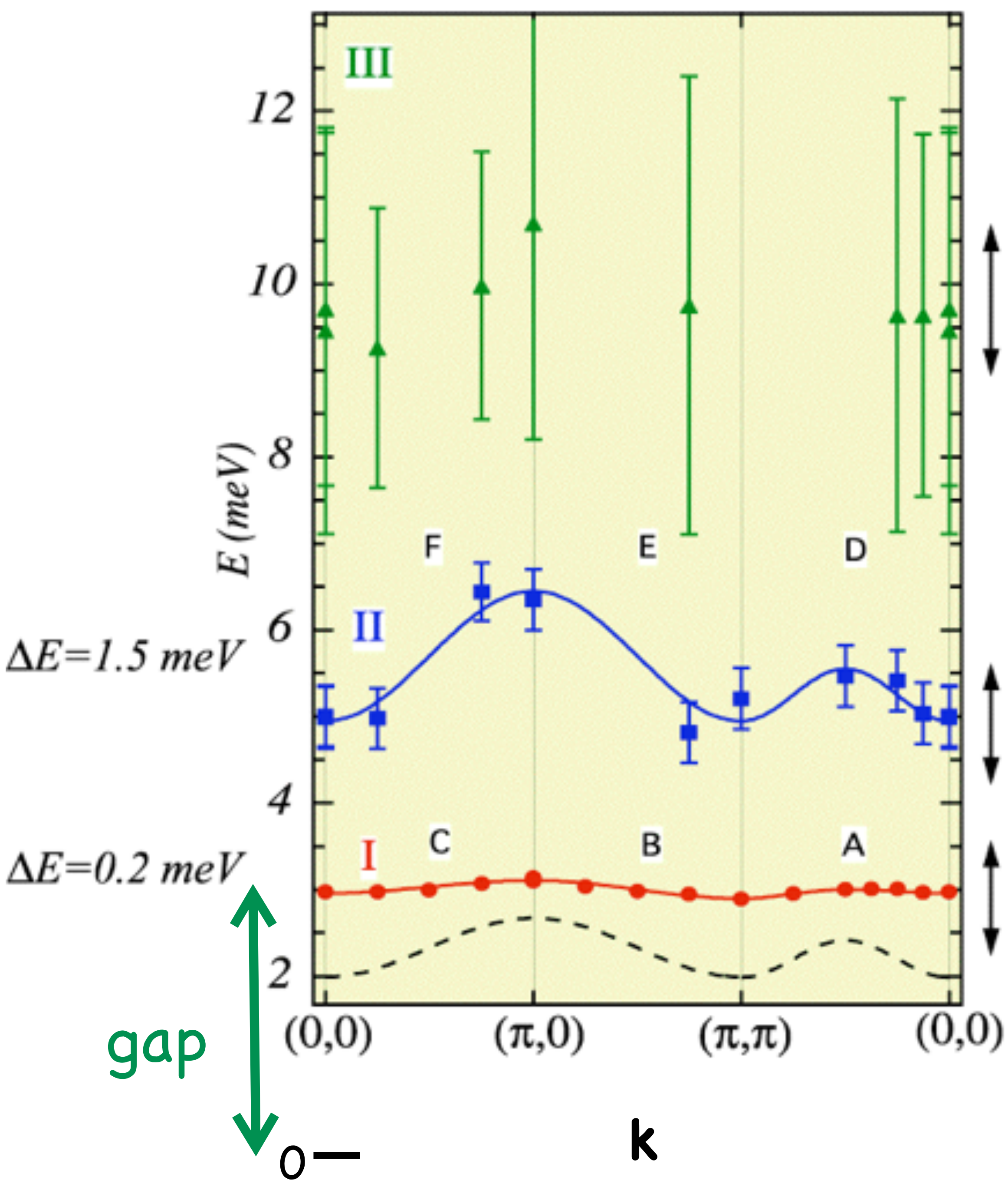

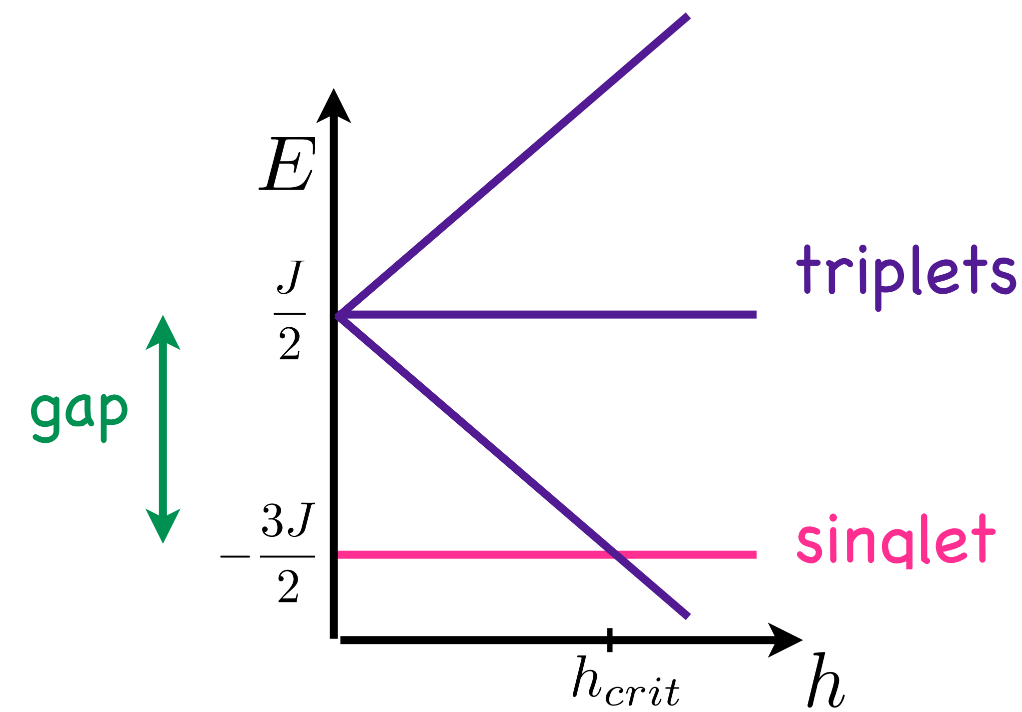

Dispersionless band of triplets

Why are triplets localized?

Why are triplets localized in orthogonal dimer systems ?

The parity of the singlet and triplet bond is different:

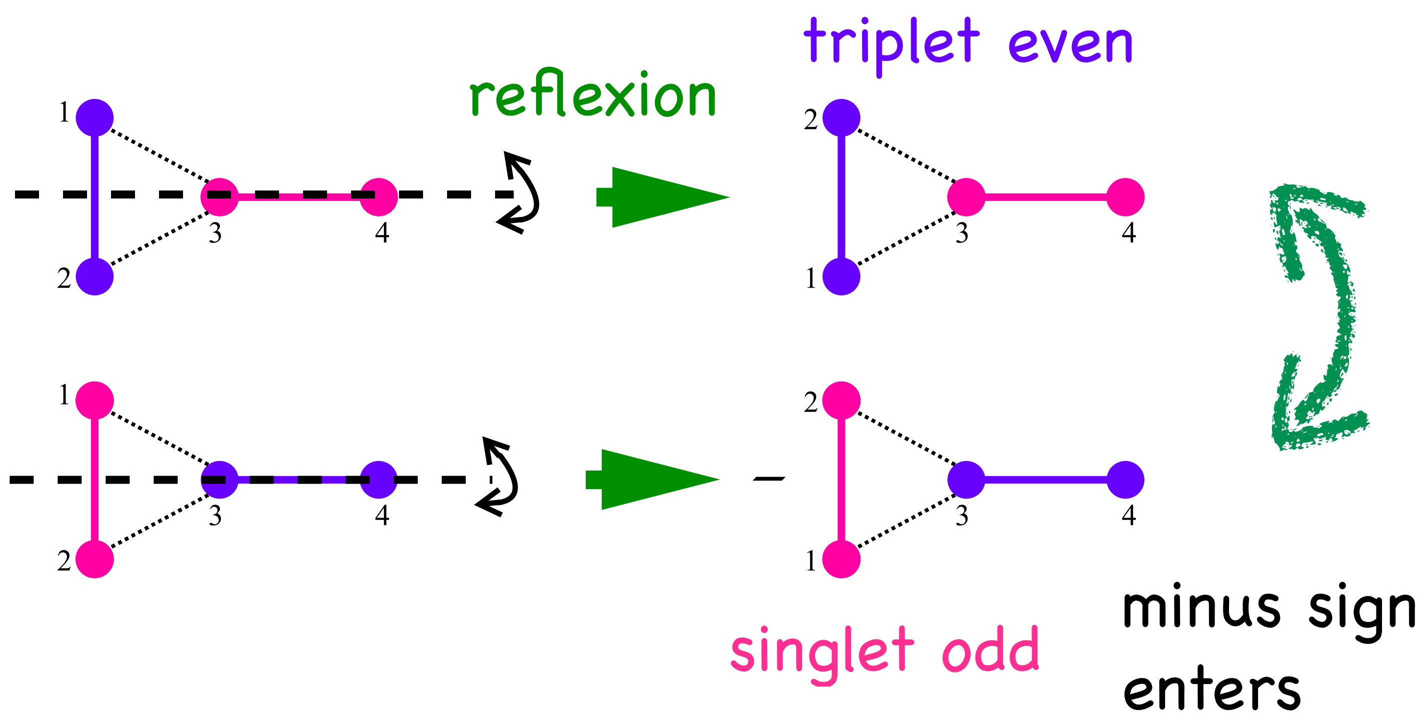

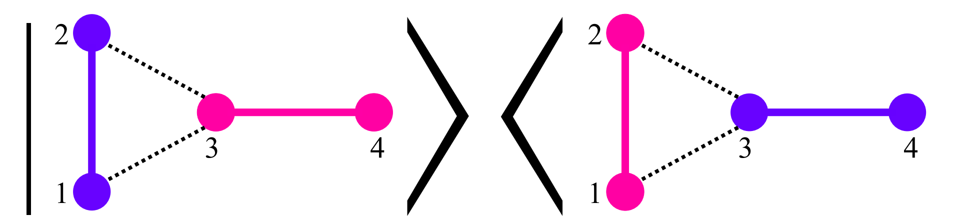

hopping matrix elements not
allowed by symmetry

a triplon can be created
next to an existing triplon

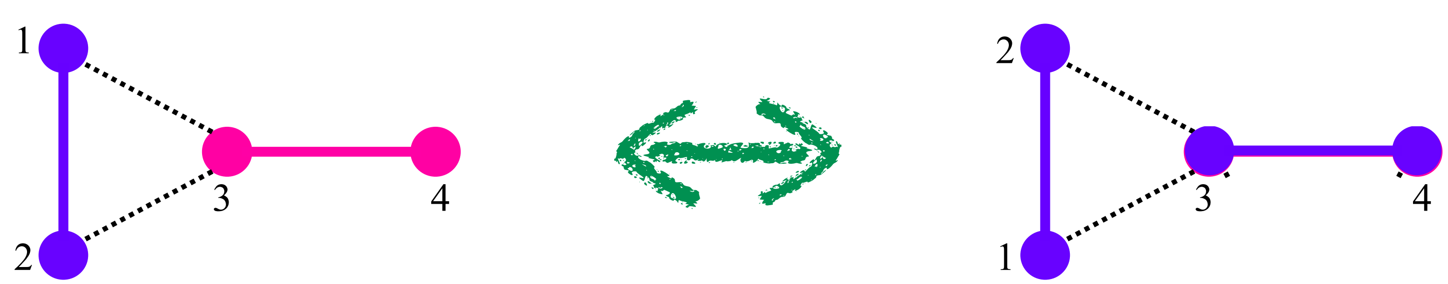

Why are triplets localized in orthogonal dimer systems ?

The parity of the singlet and triplet bond is different:

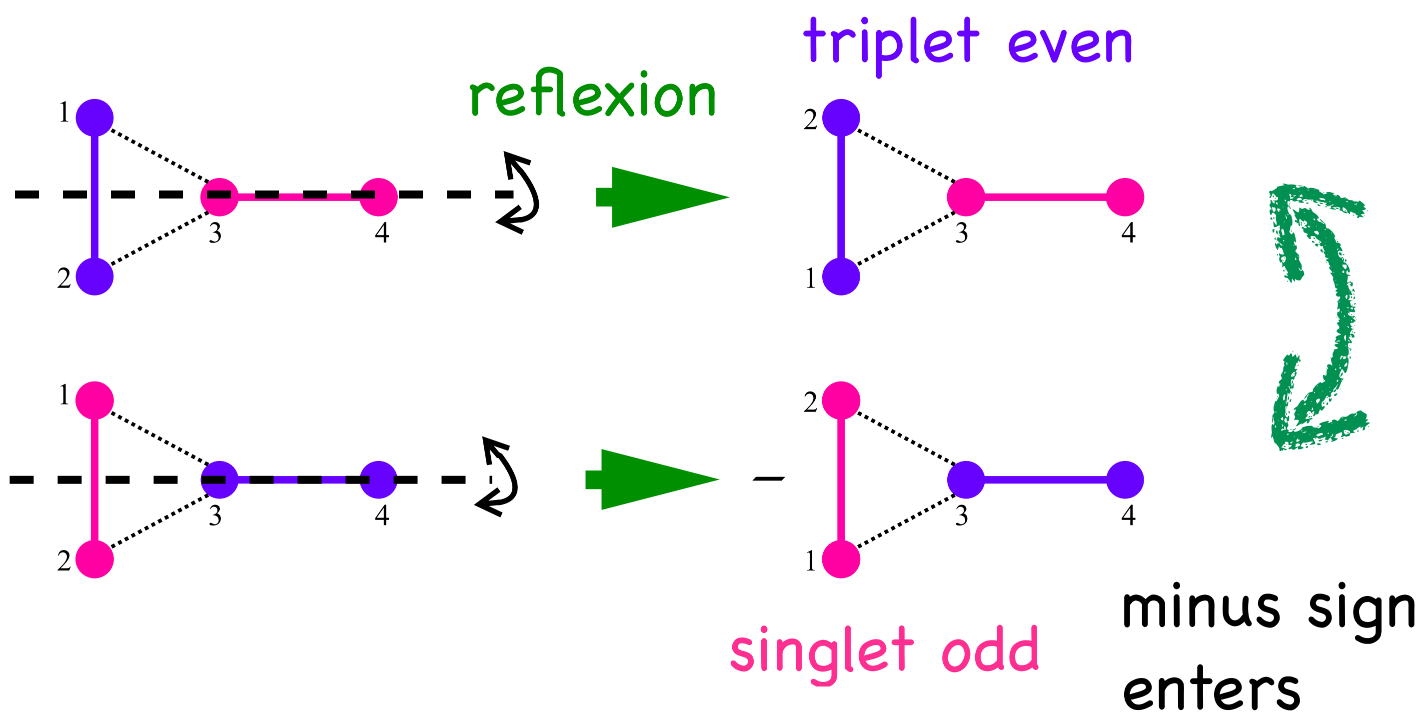

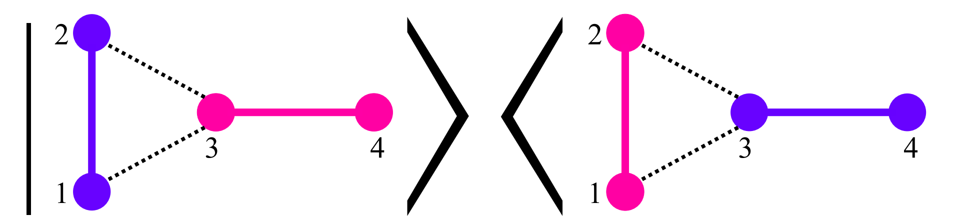

hopping matrix elements not allowed by symmetry

a 6th order process in J'/J gives a weak dispersion

S. Miyahara, K. Ueda. (2003)

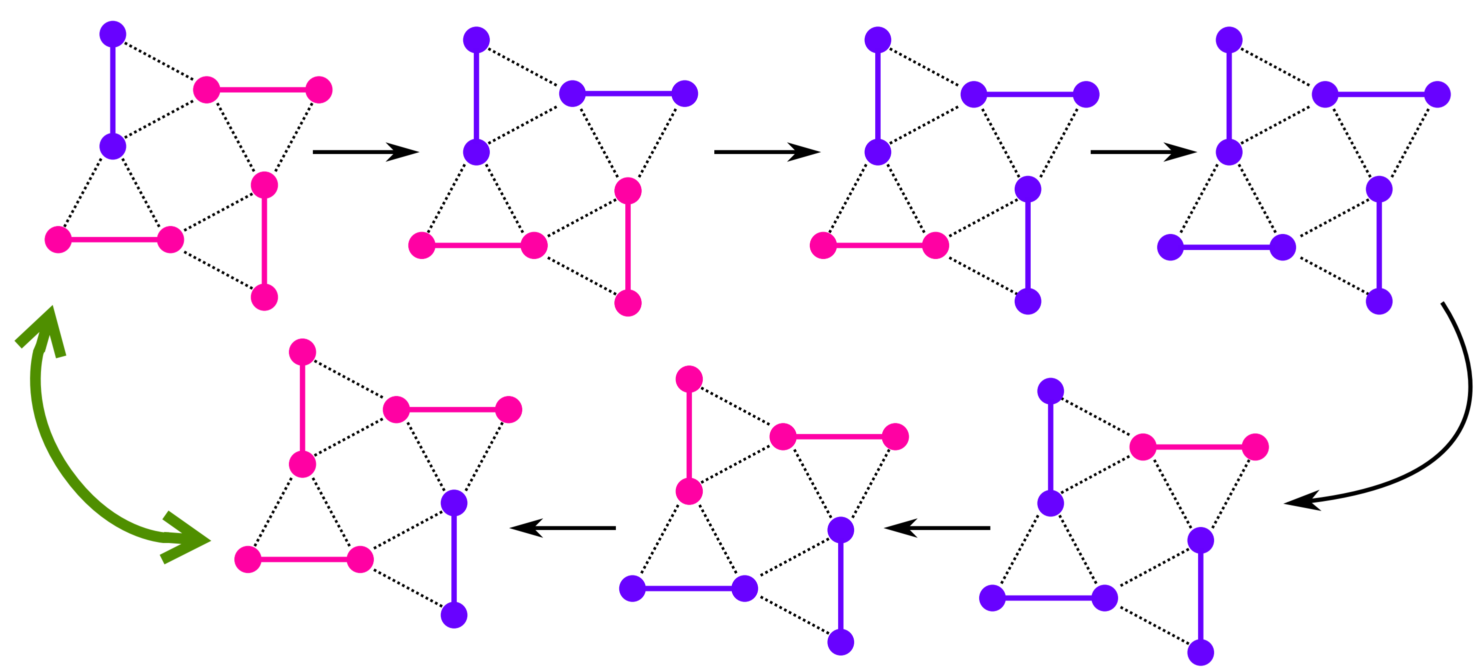

Neutron spectra

Kageyama et al., Phys. Rev. Lett. **84**, 5876 (2000)

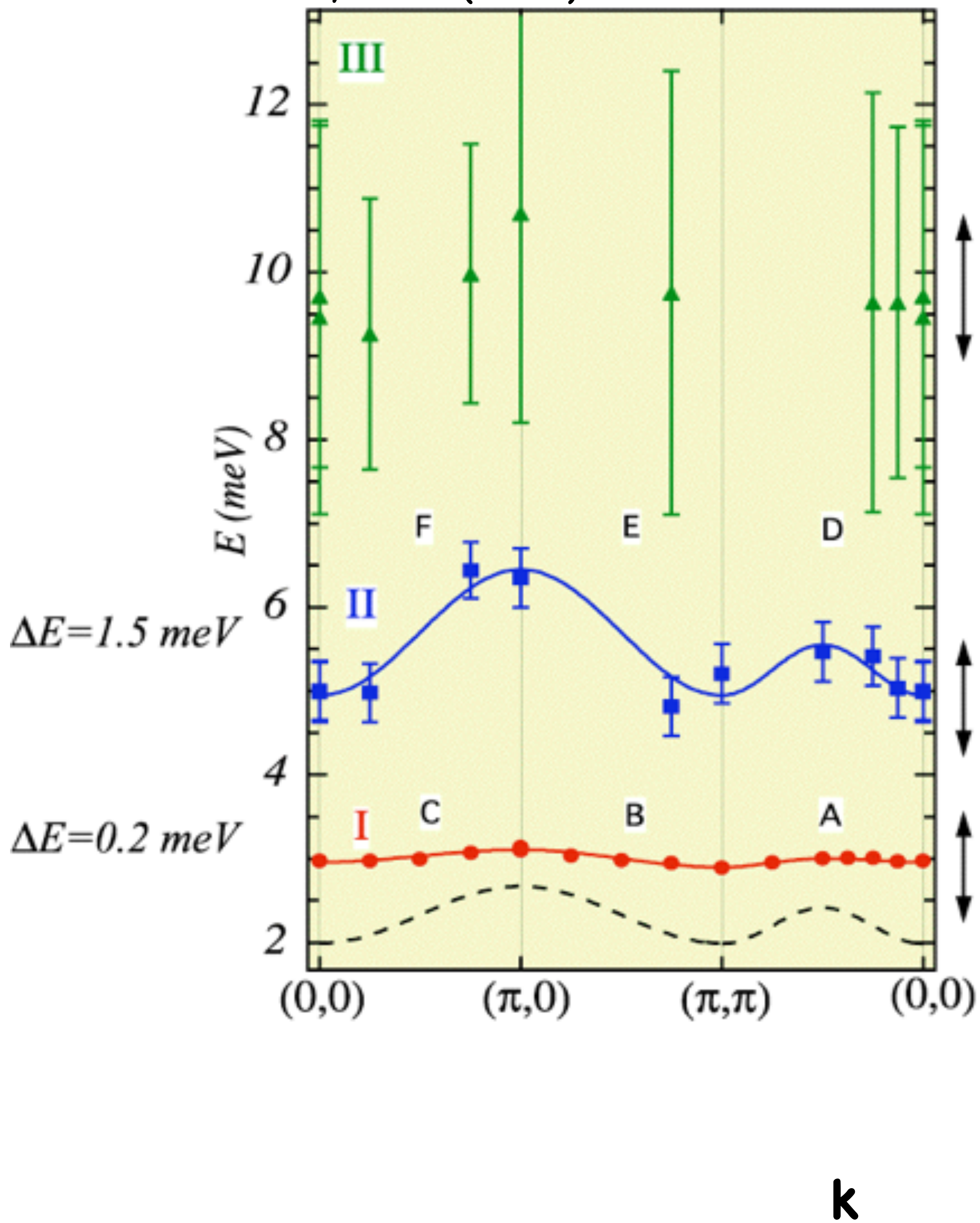

pair hopping

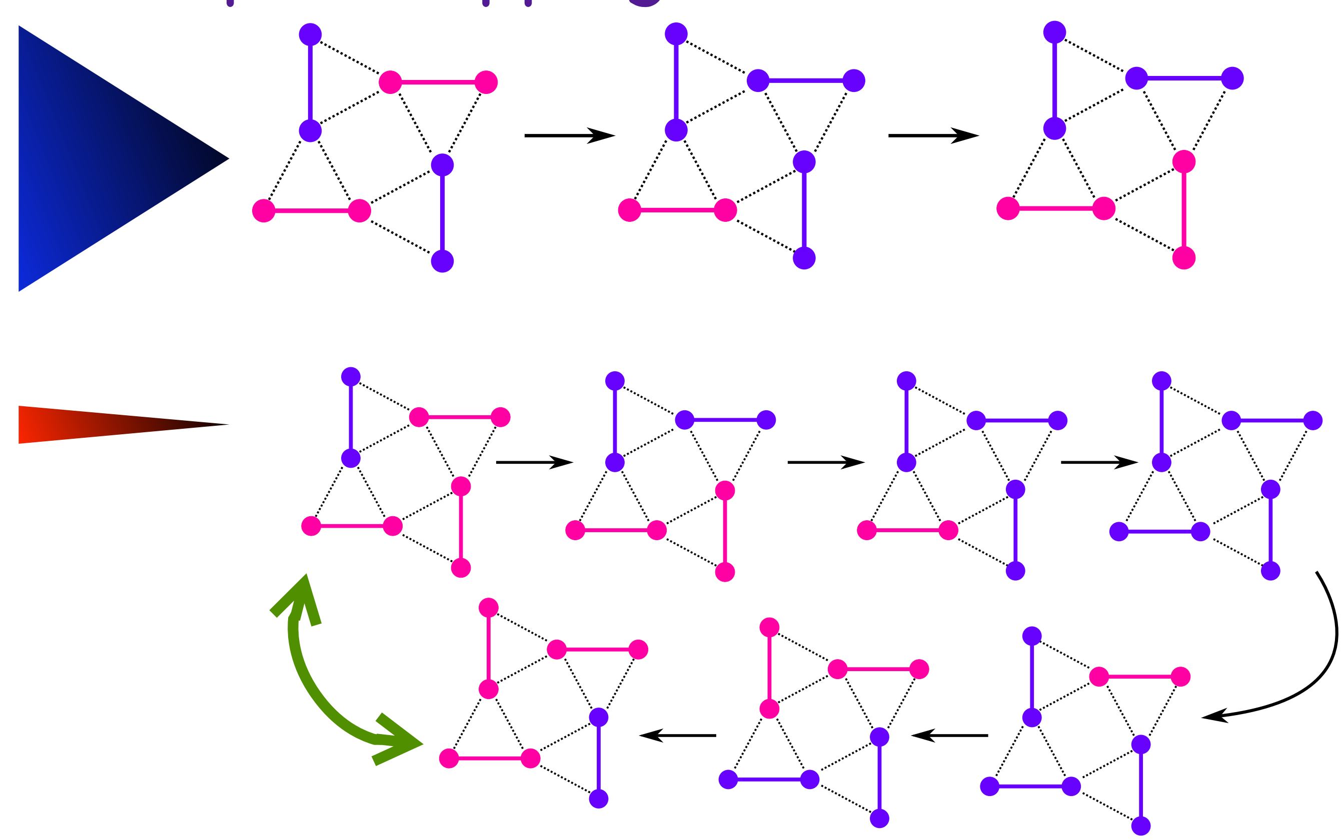

Neutron spectra - better resolution

Kageyama et al., Phys. Rev. Lett. **84**, 5876 (2000)

Even though there is no external magnetic field, the triplet excitations split. **Why ?**

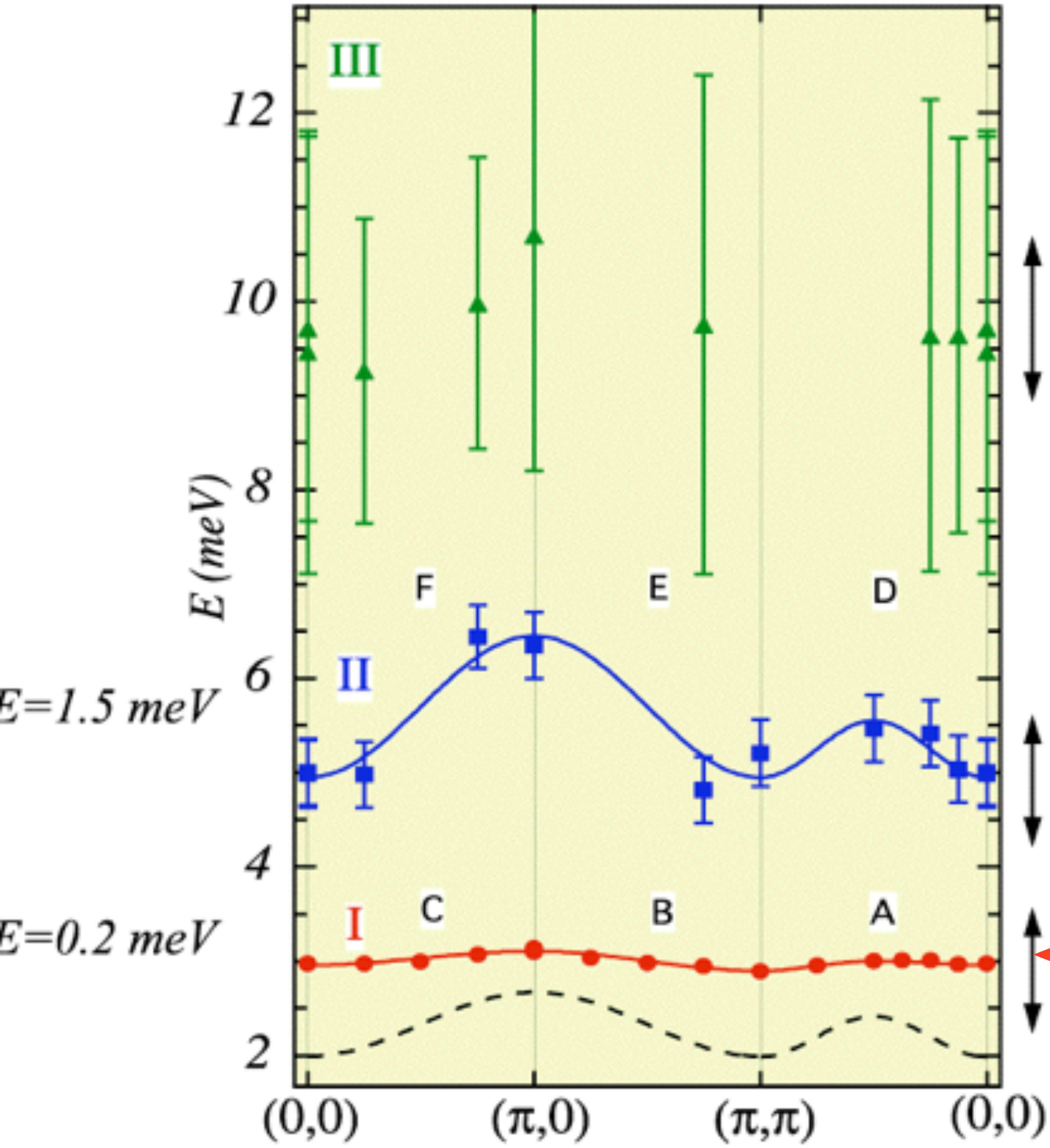

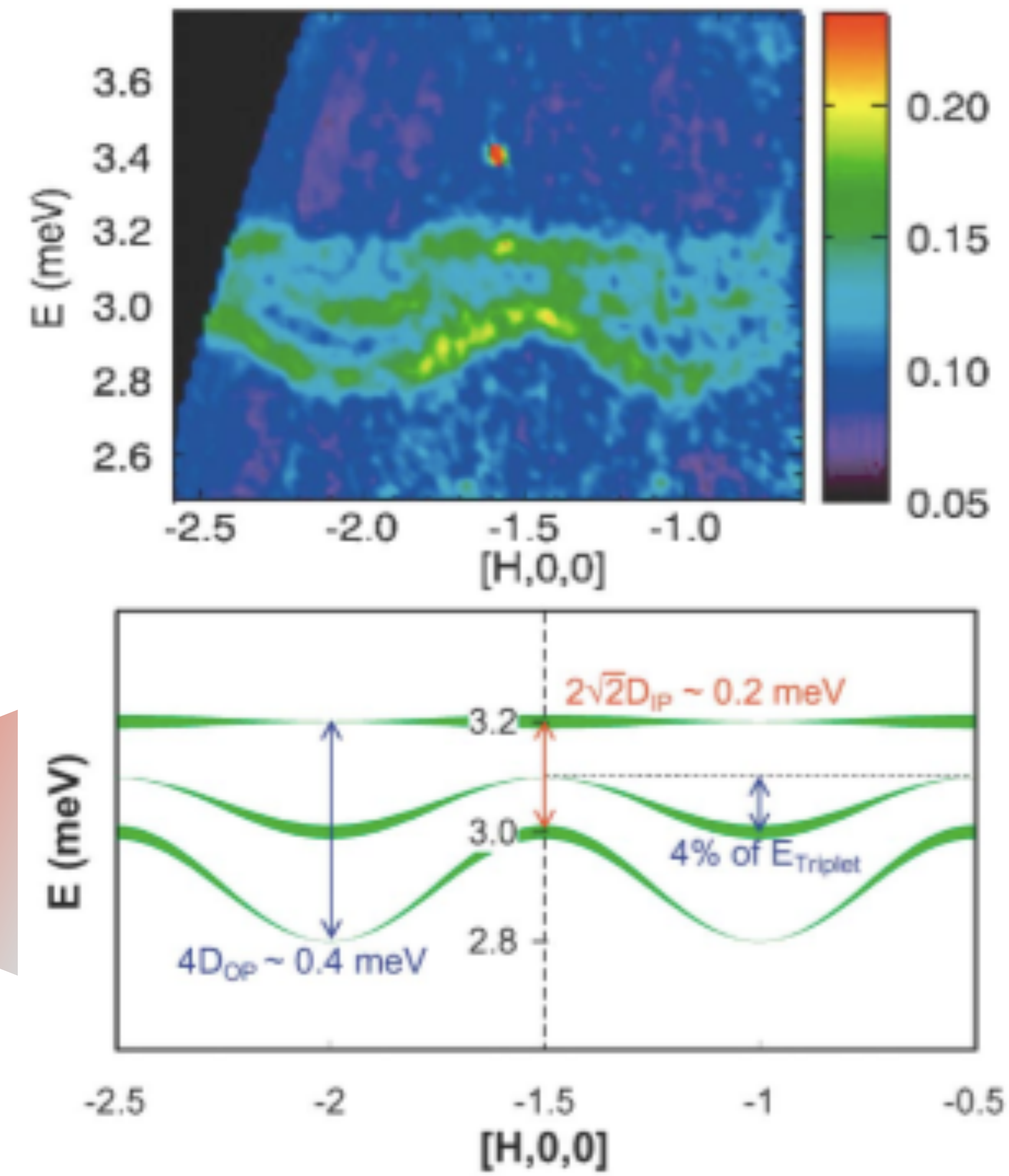

The reason: anisotropic Dzyaloshinskii-Moriya interaction

$$\mathbf{D} \sum (\mathbf{S}_i \times \mathbf{S}_j)$$

Gaulin et al. Phys. Rev. Lett. **93**, 267202 (2004)

Effects of anisotropy - ESR spectra

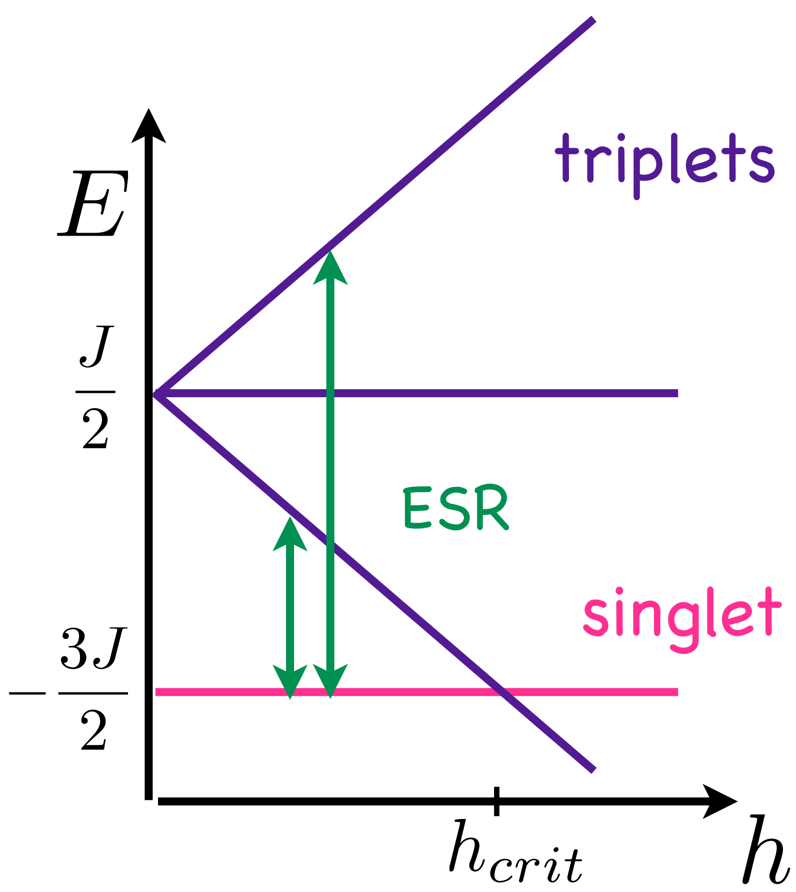

ESR: splitting of the triplets,
gap does not closes in the filed

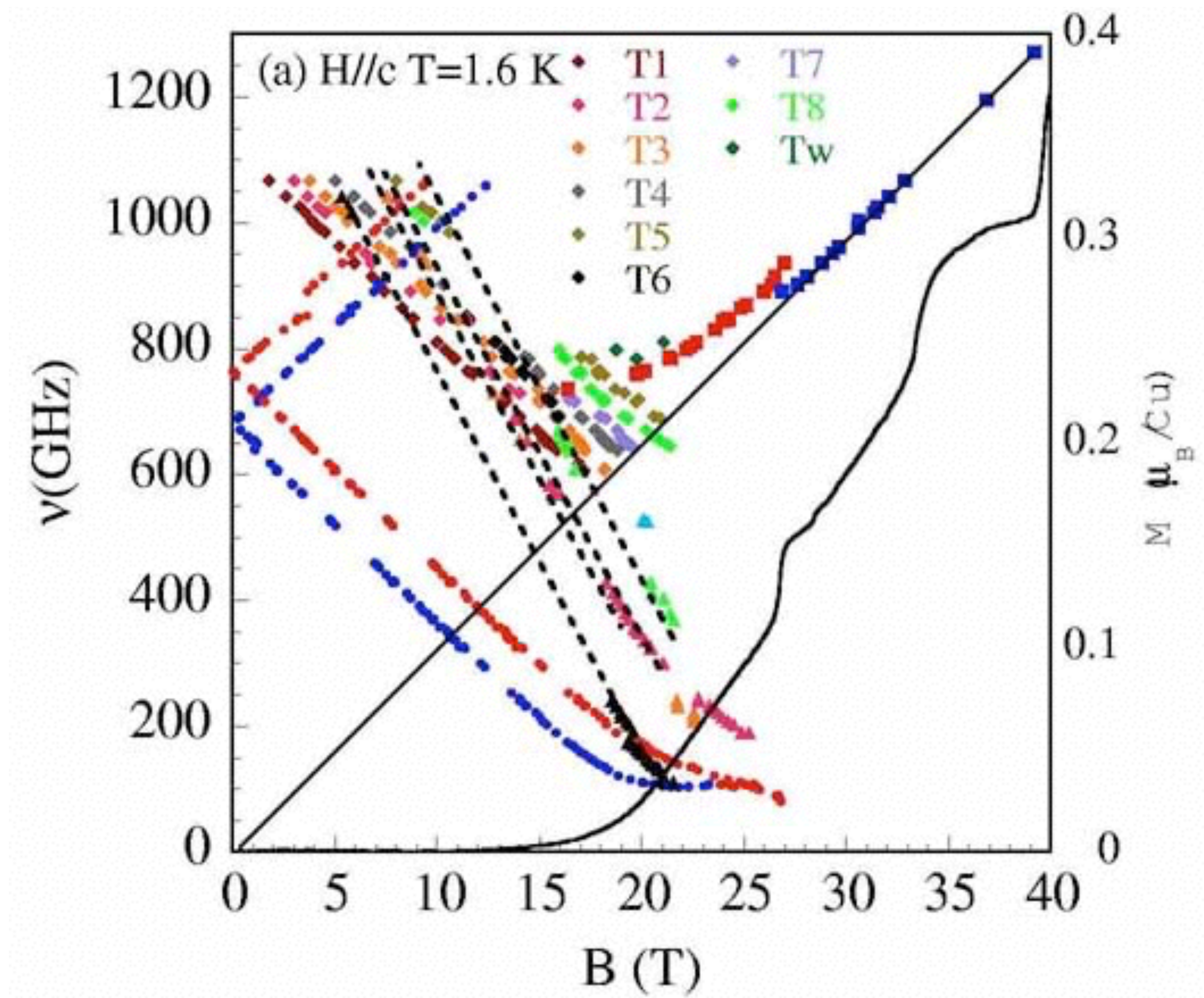

H. Nojiri, H. Kageyama, Y. Ueda and M. Motokawa
J. Phys. Soc. Japan **72**, 3243 (2003)

Effects of anisotropy - ESR, neutron, FIR spectra

Gaulin et al. Phys. Rev. Lett. **93**, 267202 (2004)

2.8 meV ≈ 680 GHz
3.2 meV ≈ 770 GHz

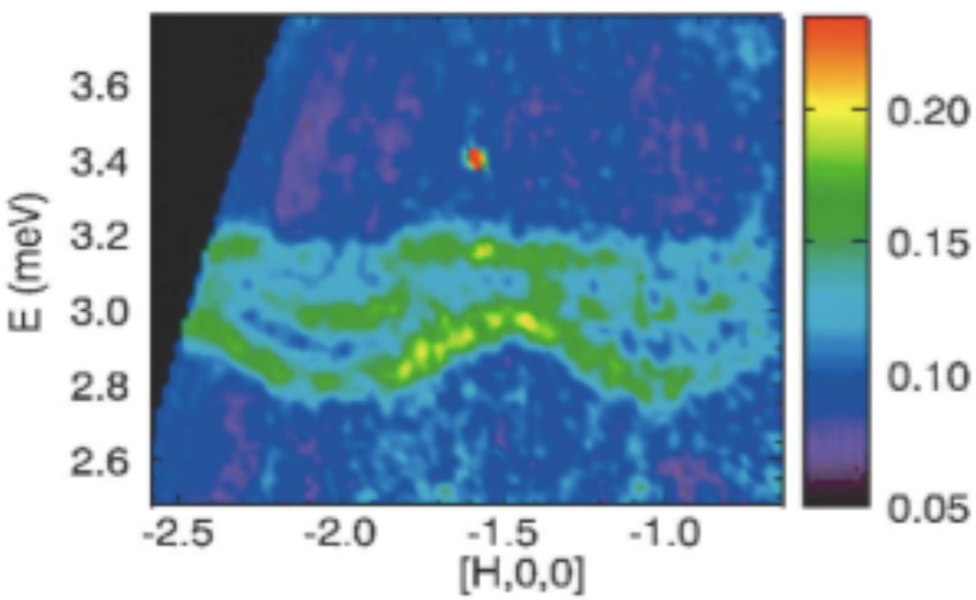

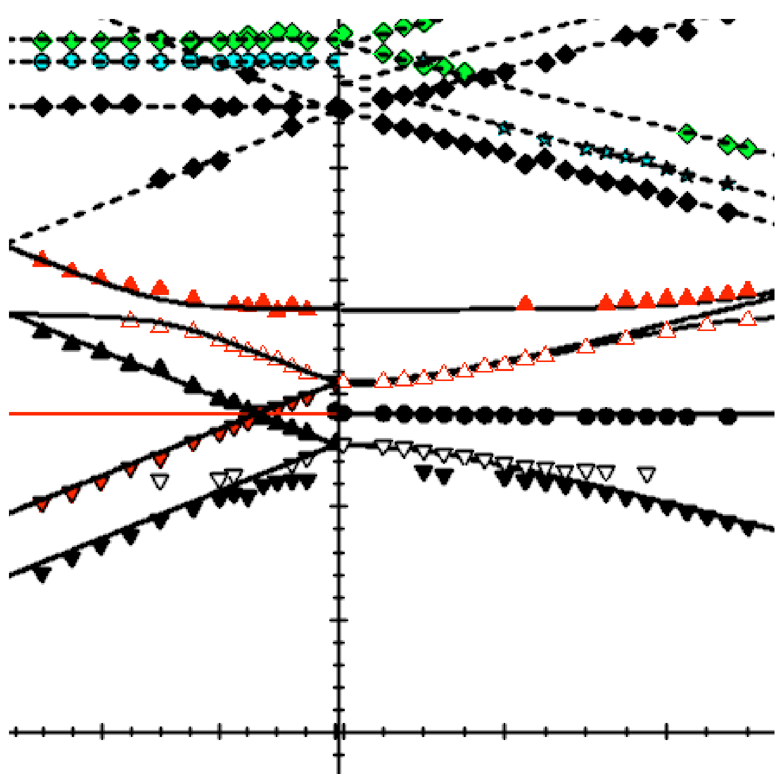

T. Rõõm et al., PRB **70**, 144417 (2004).

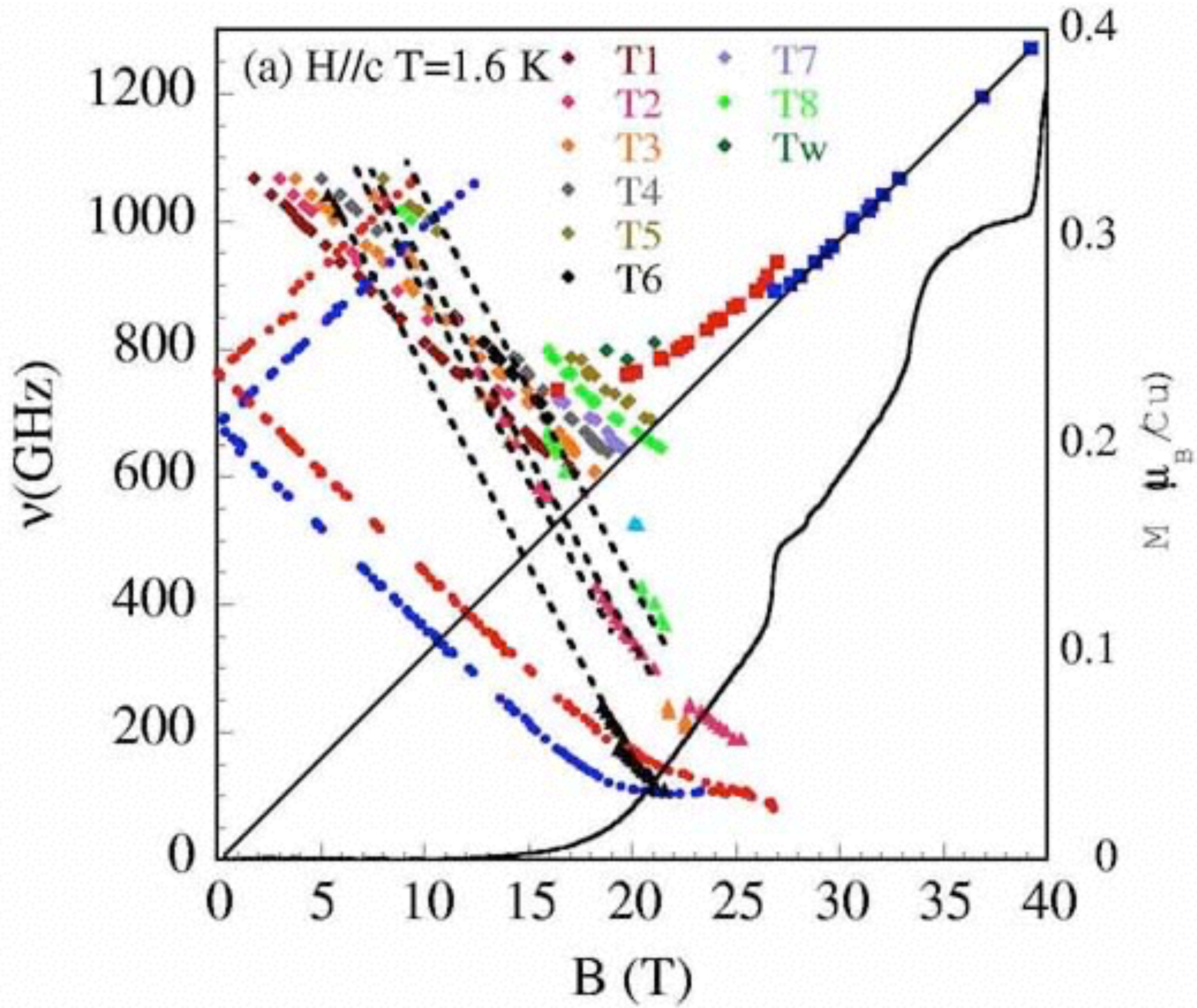

H. Nojiri, H. Kageyama, Y. Ueda and M. Motokawa J. Phys. Soc. Japan **72**, 3243 (2003)

Dzyaloshinskii's symmetry argument (1958)

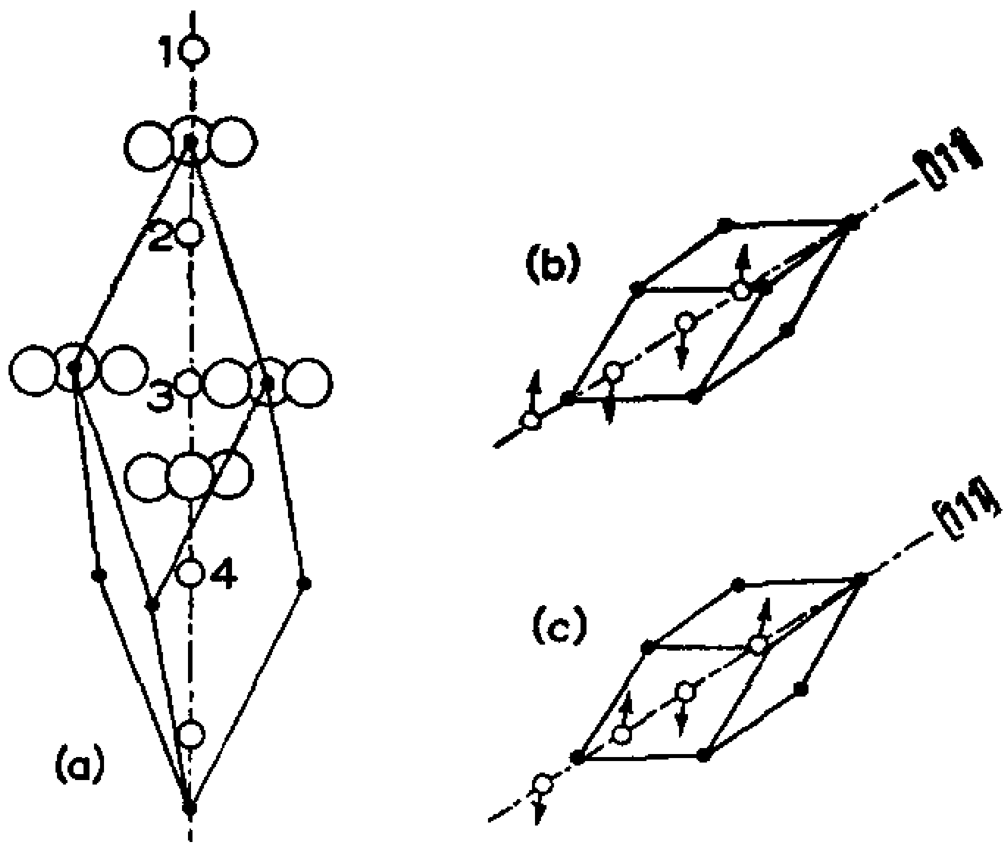

Certain antiferromagnets (α-Fe_2O_3, $CoCO_3$) show weak ferromagnetism (moment ≈ 0.02-0.0002 of full moment), sensitive to crystal symmetry. The Heisenberg Hamiltonian is not enough.

$$\mathcal{H}_{\text{Heis}} = J\mathbf{S}_1 \cdot \mathbf{S}_2$$

Dzyaloshinskii constructed the allowed spin invariants (Hamiltonian) taking into account the symmetries of the lattice.

$$\mathcal{H}_{\text{DM}} = \mathbf{D} \cdot (\mathbf{S}_1 \times \mathbf{S}_2)$$

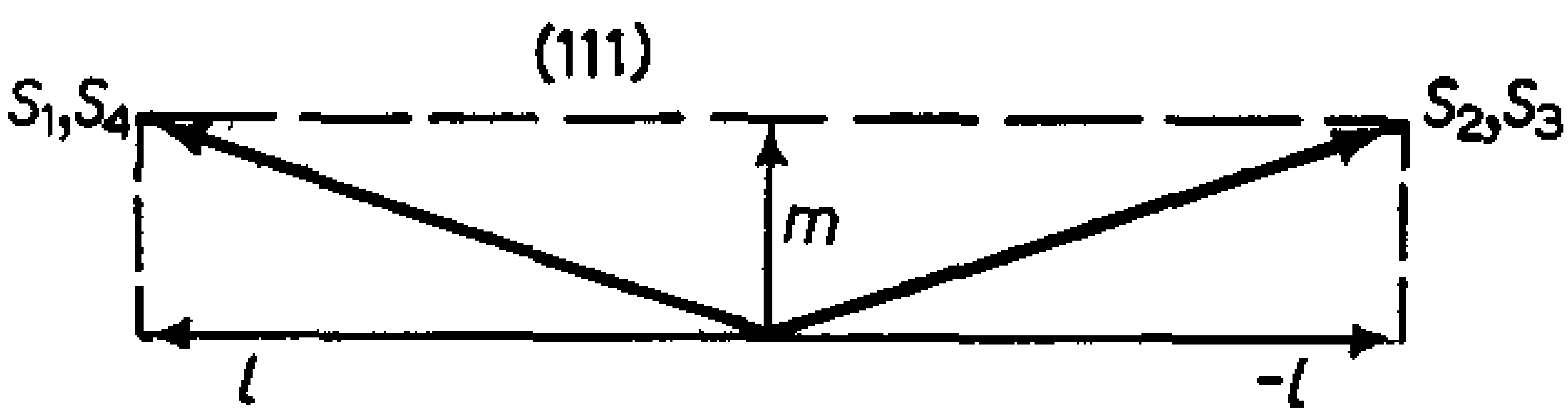

Moriya's perturbational calculation (1960)

PHYSICAL REVIEW VOLUME 120, NUMBER 1 OCTOBER 1, 1960

Anisotropic Superexchange Interaction and Weak Ferromagnetism

TÔRU MORIYA*
Bell Telephone Laboratories, Murray Hill, New Jersey
(Received May 25, 1960)

A theory of anisotropic superexchange interaction is developed by extending the Anderson theory of superexchange to include spin-orbit coupling. The antisymmetric spin coupling suggested by Dzialoshinski from purely symmetry grounds and the symmetric pseudodipolar interaction are derived. Their orders of magnitudes are estimated to be $(\Delta g/g)$ and $(\Delta g/g)^2$ times the isotropic superexchange energy, respectively. Higher order spin couplings are also discussed. As an example of antisymmetric spin coupling the case of $CuCl_2 \cdot 2H_2O$ is illustrated. In $CuCl_2 \cdot 2H_2O$, a spin arrangement which is different from one accepted so far is proposed. This antisymmetric interaction is shown to be responsible for weak ferromagnetism in α-Fe_2O_3, $MnCO_3$, and CrF_3. The paramagnetic susceptibility perpendicular to the trigonal axis is expected to increase very sharply near the Néel temperature as the temperature is lowered, as was actually observed in CrF_3.

Moriya's perturbational calculation (1960)

isotropic Heisenberg

antisymmetric

symmetric

$$E_{R,R'}^{(2)} = J_{R,R'}^{(2)}(\mathbf{S}(R)\cdot\mathbf{S}(R')) + \mathbf{D}_{R,R'}^{(2)}\cdot[\mathbf{S}(R)\times\mathbf{S}(R')] + \mathbf{S}(R)\cdot\Gamma_{R,R'}^{(2)}\cdot\mathbf{S}(R') \quad (2.3)$$

where the scalar, vector and tensor quantities: $J_{RR'}^{(2)}$, $\mathbf{D}_{R,R'}^{(2)}$, and $\Gamma_{RR'}^{(2)}$ are given in the case of one electron per ion as follows:

$$J_{R,R'}^{(2)} = 2|b_{nn'}(R-R')|^2/U, \quad (2.4a)$$

$$\mathbf{D}_{R,R'}^{(2)} = (4i/U)[b_{nn'}(R-R')\mathbf{C}_{n'n}(R'-R) - \mathbf{C}_{nn'}(R-R')b_{n'n}(R'-R)], \quad (2.4b)$$

$$\Gamma_{RR'}^{(2)} = (4/U)[\mathbf{C}_{nn'}(R-R')\mathbf{C}_{n'n}(R'-R) + \mathbf{C}_{n'n}(R'-R)\mathbf{C}_{nn'}(R-R') - (\mathbf{C}_{nn'}(R-R')\cdot\mathbf{C}_{n'n}(R'-R))1]. \quad (2.4c)$$

$$D\sim(\Delta g/g)J, \quad \Gamma\sim(\Delta g/g)^2 J.$$

Symmetry point group of $SrCu_2(BO_3)_2$

p4g high symmetry wallpaper group (above T_s=395K)

Wikipedia:

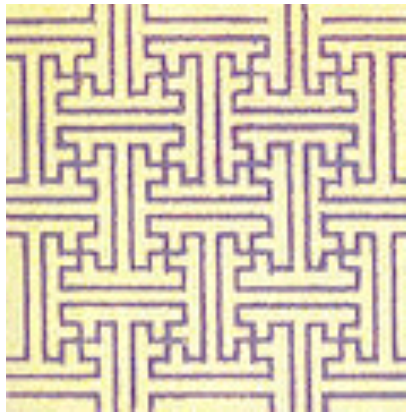

paintings from China

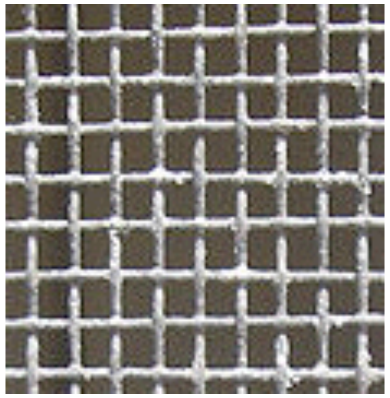

fly screen from US

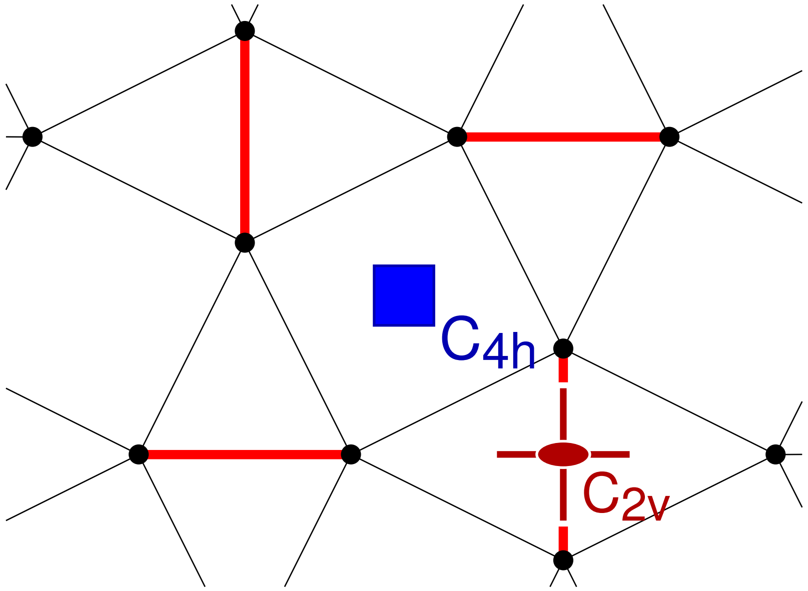

cmm low symmetry wallpaper group (below T_s=395K)

painting from an egyptian tomb

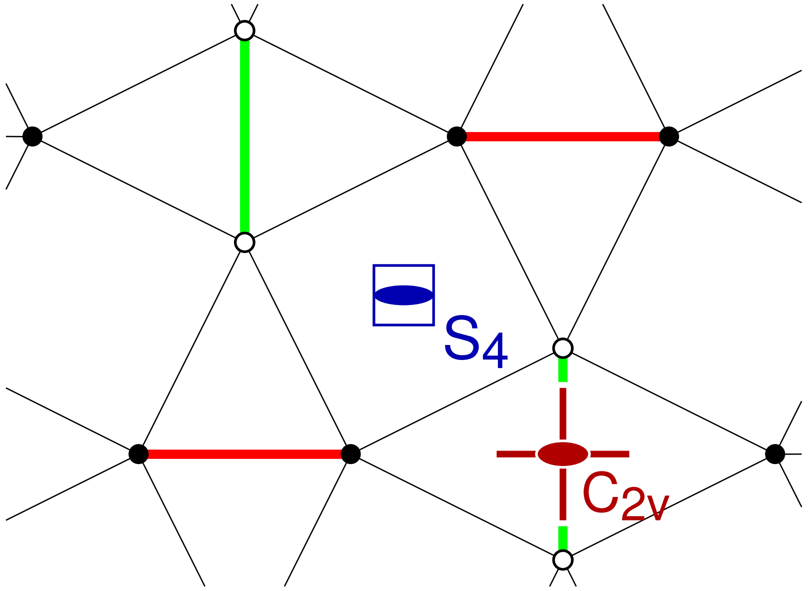

DM - interactions allowed by the symmetry

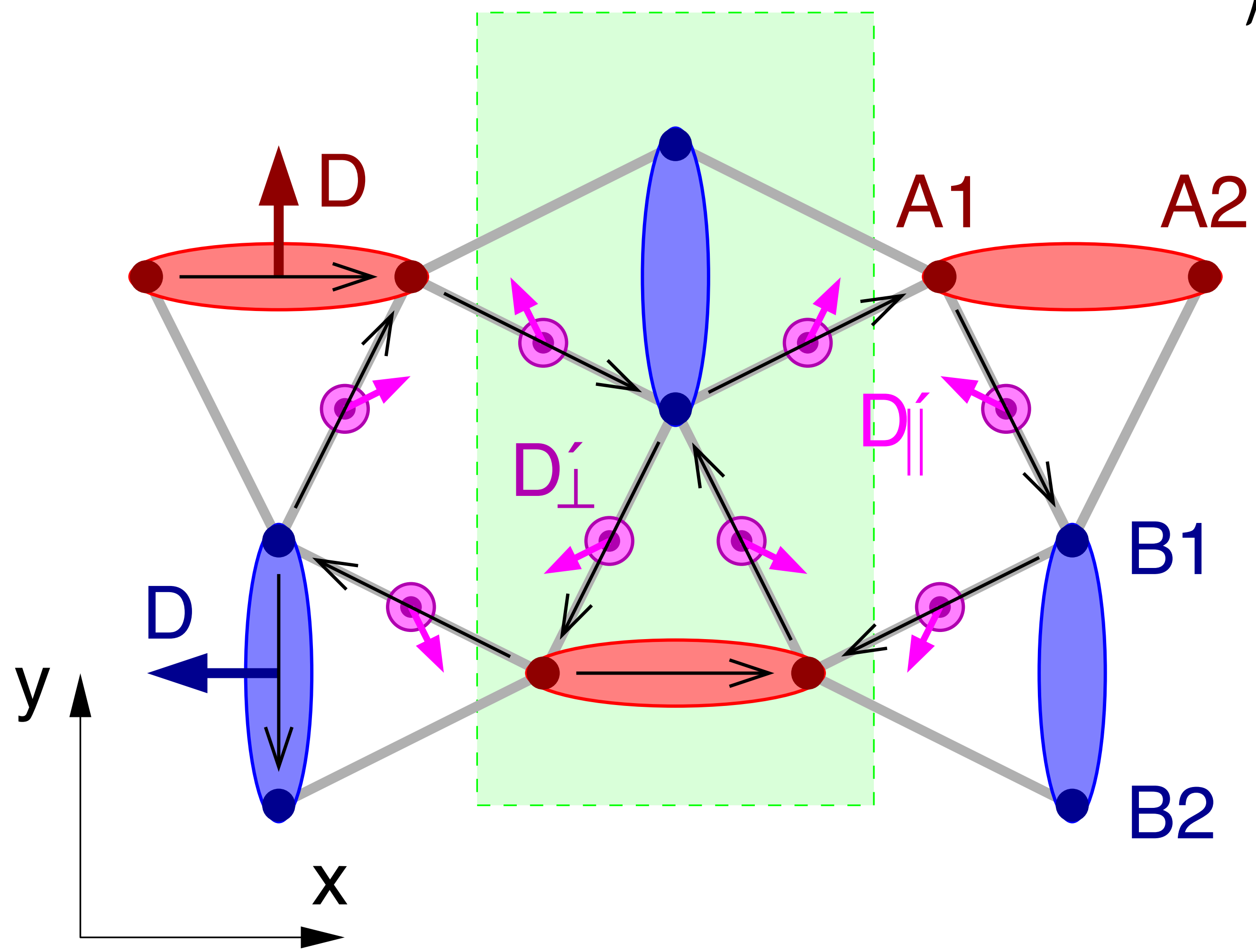

$$\mathcal{H} = J \sum_{nn} \mathbf{S}_i \mathbf{S}_j + J' \sum_{nnn} \mathbf{S}_i \mathbf{S}_j - h_\alpha \sum_j \mathbf{S}_j^\alpha$$
$$+ \mathbf{D} \sum_{nn} (\mathbf{S}_i \times \mathbf{S}_j) + \mathbf{D}' \sum_{nnn} (\mathbf{S}_i \times \mathbf{S}_j)$$

Low symmetry phase (T< 395K):

intradimer: D

interdimer: $D'_\perp$ $D'_{\|ns}$ $D'_{\|s}$

e.g. K Kodama et al., J. Phys.: Condensed Matt **17,** L61 (2005)

Shastry-Sutherland model + DM interaction

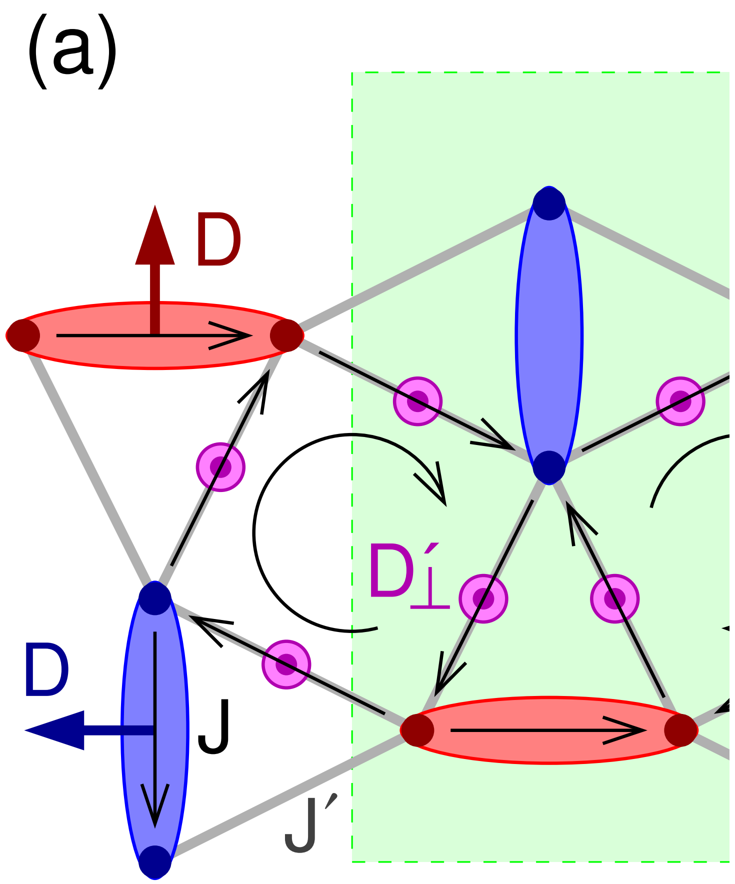

$$\mathcal{H} = J\sum_{n.n.}\mathbf{S}_i\cdot\mathbf{S}_j + J'\sum_{n.n.n.}\mathbf{S}_i\cdot\mathbf{S}_j - h_z\sum_i S_i^z + \sum_{\text{n.n.}}\mathbf{D}_{ij}\cdot(\mathbf{S}_i\times\mathbf{S}_j) + \sum_{\text{n.n.n.}}\mathbf{D}'_{ij}\cdot(\mathbf{S}_i\times\mathbf{S}_j)$$

Ground state: $|\Psi\rangle = \prod |\tilde{s}\rangle_A|\tilde{s}\rangle_B$

$$|\tilde{s}\rangle_A = |s\rangle_A + \lambda|t_y\rangle_A$$
$$|\tilde{s}\rangle_B = |s\rangle_B - \lambda|t_x\rangle_B$$

$E_0 = \frac{\langle\Psi|\mathcal{H}|\Psi\rangle}{\langle\Psi|\Psi\rangle}$ minimization gives $\lambda = -\frac{D}{2J}$

JR et al PRB **83** 024413 (2011)

the new triplet basis:

$$|\tilde{t}_x\rangle_A = |t_x\rangle_A \qquad |\tilde{t}_x\rangle_B = \lambda|s\rangle_B + |t_x\rangle_B$$
$$|\tilde{t}_y\rangle_A = -\lambda|s\rangle_A + |t_y\rangle_A \qquad |\tilde{t}_y\rangle_B = |t_y\rangle_B$$
$$|\tilde{t}_z\rangle_A = |t_z\rangle_A \qquad |\tilde{t}_z\rangle_B = |t_z\rangle_B$$

$$|t_x\rangle = \frac{i}{\sqrt{2}}(|\uparrow\uparrow\rangle - |\downarrow\downarrow\rangle)$$
$$|t_y\rangle = \frac{1}{\sqrt{2}}(|\uparrow\uparrow\rangle + |\downarrow\downarrow\rangle)$$
$$|t_z\rangle = -\frac{i}{\sqrt{2}}(|\uparrow\downarrow\rangle + |\downarrow\uparrow\rangle)$$

correspond to the 6 different ‘triplet’-like excitation

The variational approach and bond-wave spectra

Step 1: we minimize the energy with a dimer-product variational wave function (entanglement within dimers taken care of):

$$|\Psi\rangle = \prod_{\text{bonds}} (\alpha_s |s\rangle + \alpha_1 |t_1\rangle + \alpha_0 |t_0\rangle + \alpha_{\bar{1}} |t_{\bar{1}}\rangle)(\beta_s |s\rangle + \beta_1 |t_1\rangle + \beta_0 |t_0\rangle + \beta_{\bar{1}} |t_{\bar{1}}\rangle)$$

Step 2: starting from the variational solution, we construct a bond-wave hamiltonian analogous to the spin-wave approach:

$$\begin{aligned} S^{\alpha}_{j,1} &= \frac{i}{2}\left(t^{\dagger}_{\alpha,j} s_j - s^{\dagger}_j t_{\alpha,j}\right) - \frac{i}{2}\epsilon_{\alpha,\beta,\gamma} t^{\dagger}_{\beta,j} t_{\gamma,j} \, , \\ S^{\alpha}_{j,2} &= -\frac{i}{2}\left(t^{\dagger}_{\alpha,j} s_j - s^{\dagger}_j t_{\alpha,j}\right) - \frac{i}{2}\epsilon_{\alpha,\beta,\gamma} t^{\dagger}_{\beta,j} t_{\gamma,j} \, . \end{aligned}$$

s and t_μ bosons are like Schwinger-bosons, and condensing one boson (variational solution) we get the Holstein-Primakoff representation and a 1/M expansion:

$$s^{\dagger}, s \;\approx\; \sqrt{M - \sum_{\mu} t^{\dagger}_{\mu} t_{\mu}} \approx M - \frac{1}{2M} \sum_{\mu} t^{\dagger}_{\mu} t_{\mu}$$

quadratic Hamiltonian which can be Bogoliubov diagolized:

$$\mathcal{H}^{(2)} = \frac{1}{2} \sum_{\mathbf{k}\in \mathrm{BZ}} \begin{pmatrix} \tilde{\mathbf{t}}^{\dagger}_{\mathbf{k}} \\ \tilde{\mathbf{t}}_{-\mathbf{k}} \end{pmatrix}^{T} \begin{pmatrix} M & N \\ N^{*} & M \end{pmatrix} \begin{pmatrix} \tilde{\mathbf{t}}_{\mathbf{k}} \\ \tilde{\mathbf{t}}^{\dagger}_{-\mathbf{k}} \end{pmatrix}$$

Comparison with experiments: neutron spectra at H=0

bond-wave result:

see also: Y. F. Cheng, PRB 75, 144422 (2007)

$$\omega_{\mathbf{q}} = \sqrt{J^2 \pm J\Omega_{\mathbf{q}}} \approx J \pm \frac{1}{2}\Omega_{\mathbf{q}}$$

$$\Omega_{\mathbf{q}} = \left[\left(\frac{J'D}{J} - 2D'_{||,s}\right)^2 (1-\cos a \cos b) + 16 D'^2_{\perp} \cos^2\frac{a}{2}\cos^2\frac{b}{2}\right]^{1/2}$$

J. Romhányi, K. Totsuka, K. Penc,
Phys. Rev. B **83**, 024413 (2011).

B. Gaulin et al.,
PRL **93**, 267202 (2004)

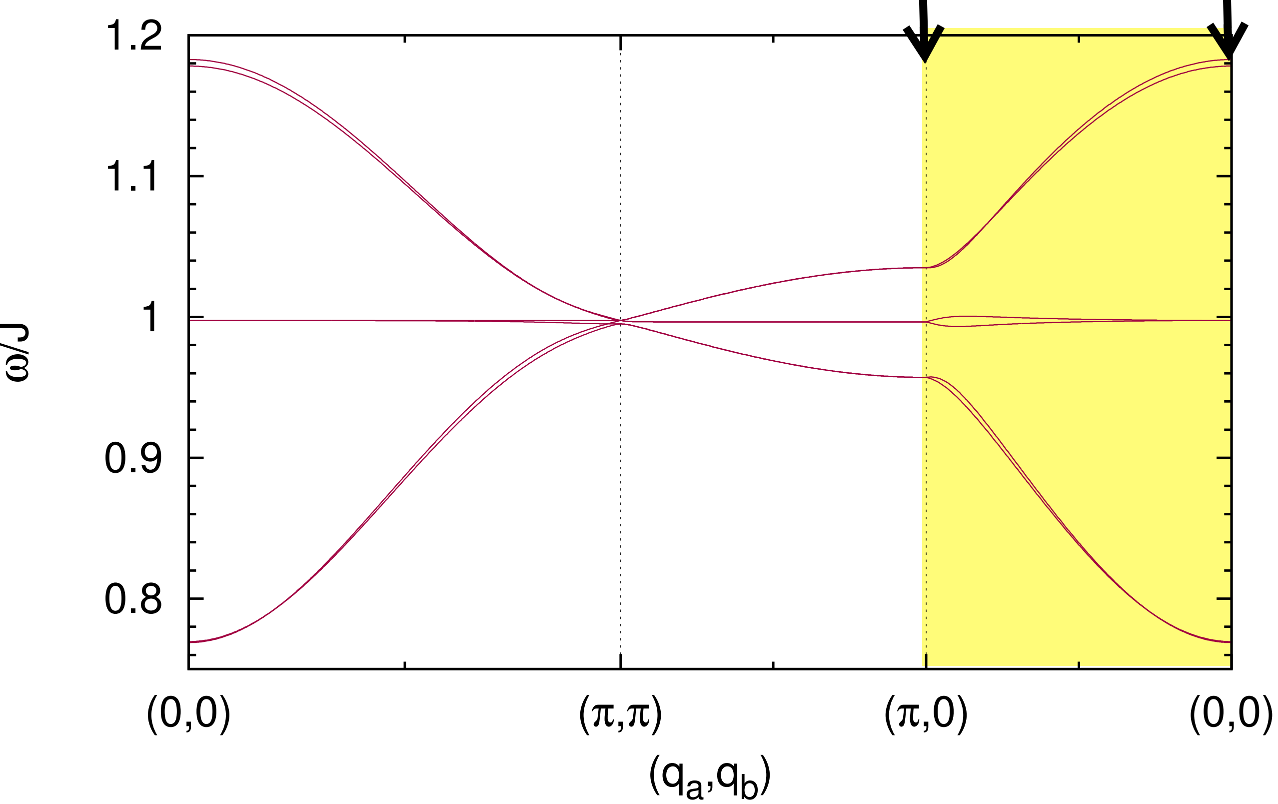

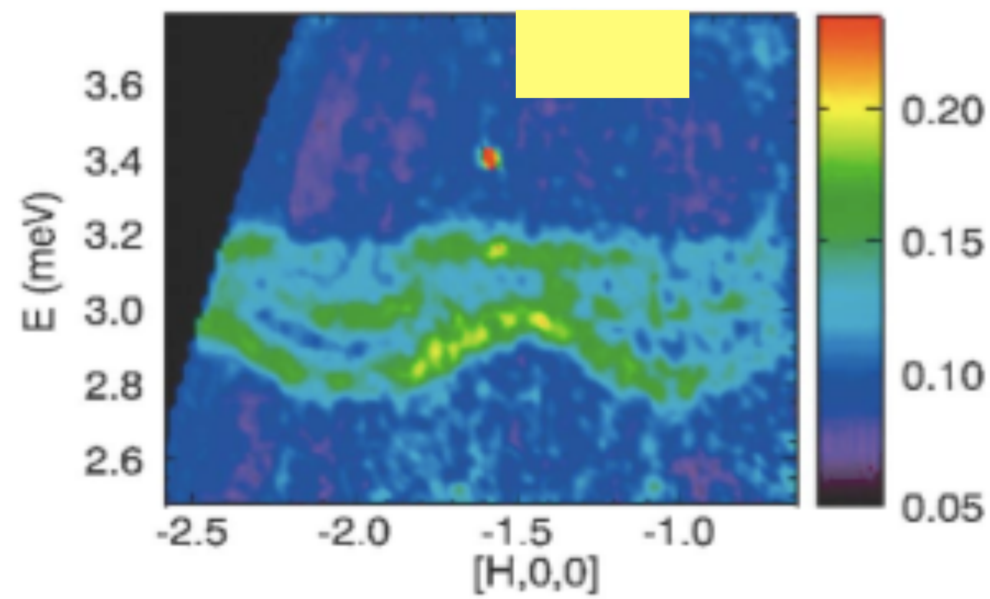

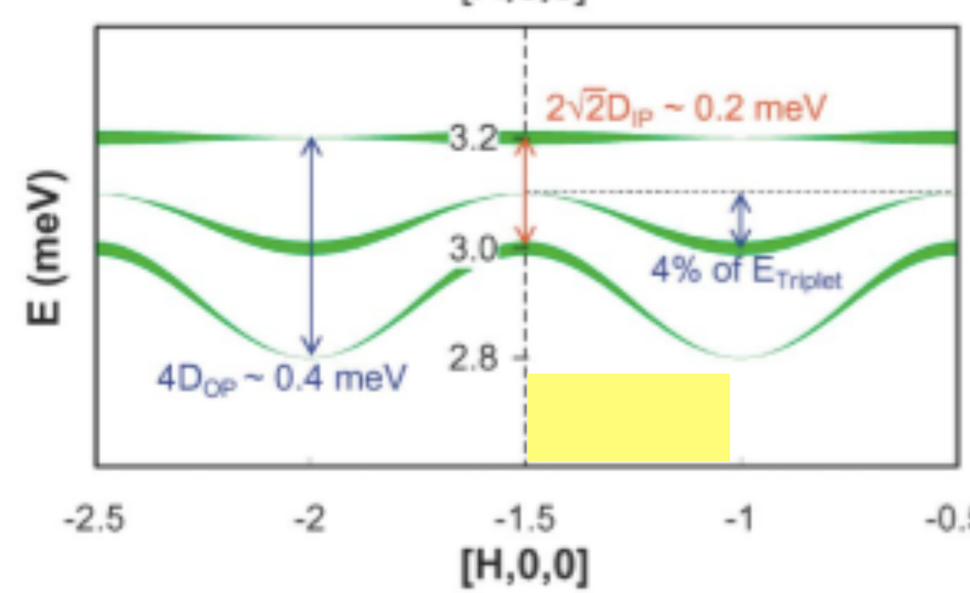

The triplet dispersion due to J' (6th order process) are missing from our treatment.

Quantitative comparison with measured ESR & IR spectra: gap in the field

[J. Romhányi, K. Totsuka, K. Penc, Phys. Rev. B **83**, 024413 (2011).]

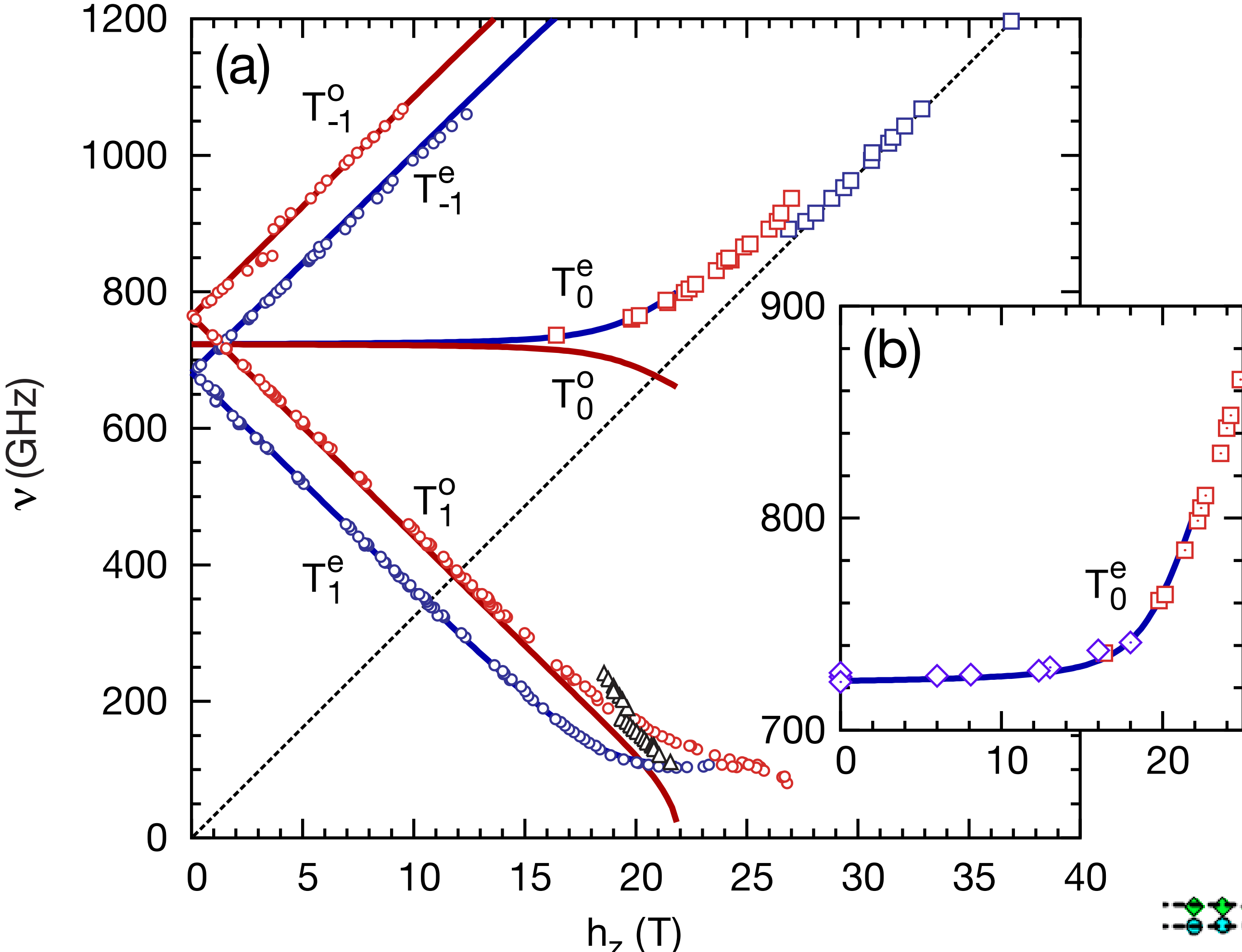

H. Nojiri, H. Kageyama, Y. Ueda and M. Motokawa

J. Phys. Soc. Japan **72**, 3243 (2003)

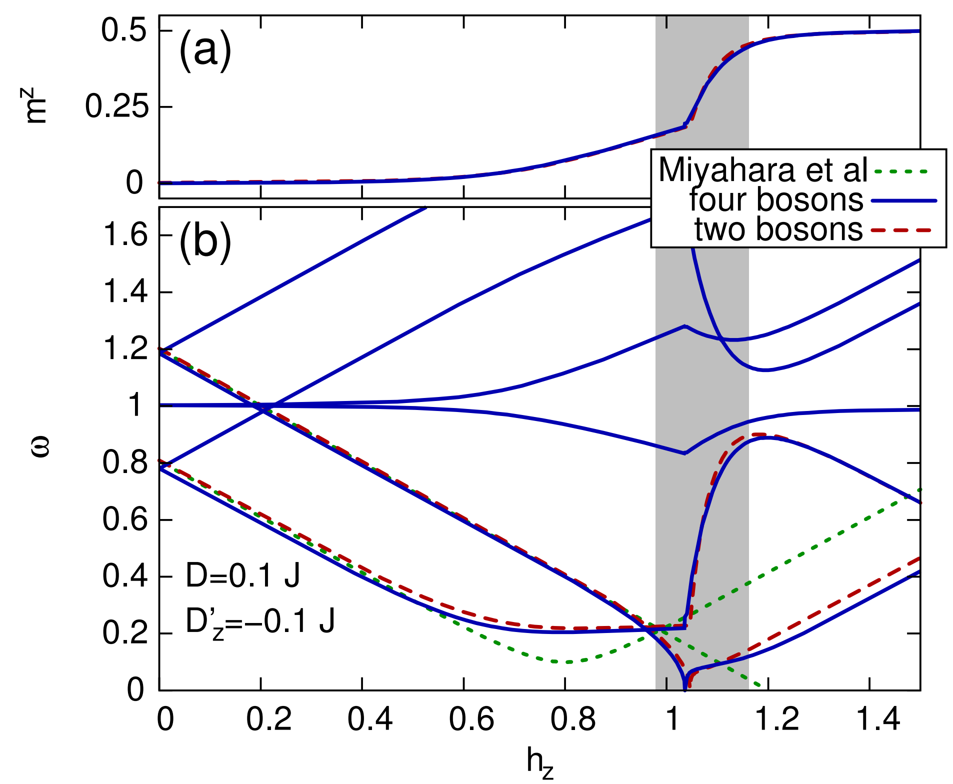

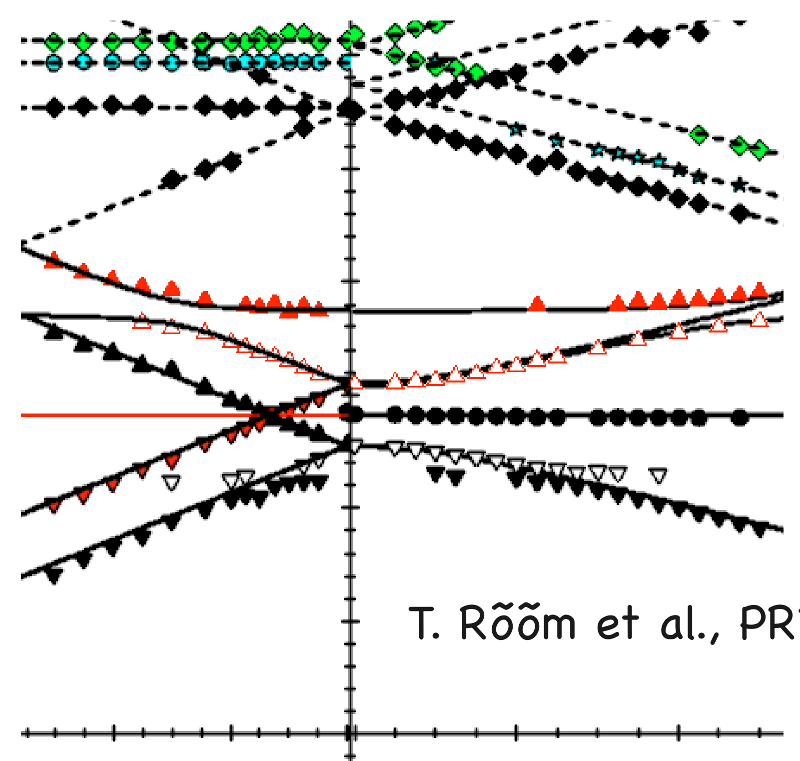

T. Rõõm et al., PRB **70**, 144417 (2004).

Hamiltonian describing the hopping of triplets

assuming that $h, D, D'_\perp \ll J, J'$

$$\mathcal{H} = \begin{pmatrix} \tilde{t}^\dagger_{x,B,\mathbf{k}} \\ \tilde{t}^\dagger_{y,B,\mathbf{k}} \\ \tilde{t}^\dagger_{z,B,\mathbf{k}} \\ \tilde{t}^\dagger_{x,A,\mathbf{k}} \\ \tilde{t}^\dagger_{y,A,\mathbf{k}} \\ \tilde{t}^\dagger_{z,A,\mathbf{k}} \end{pmatrix}^T \begin{pmatrix} J & ih_z & 0 & 0 & -2D'_\perp\gamma_1 & -\frac{iDJ'\gamma_3}{2J} \\ -ih_z & J & 0 & 2D'_\perp\gamma_1 & 0 & -\frac{iDJ'\gamma_2}{2J} \\ 0 & 0 & J & \frac{iDJ'\gamma_3}{2J} & \frac{iDJ'\gamma_2}{2J} & 0 \\ 0 & 2D'_\perp\gamma_1 & -\frac{iDJ'\gamma_3}{2J} & J & ih_z & 0 \\ -2D'_\perp\gamma_1 & 0 & -\frac{iDJ'\gamma_2}{2J} & -ih_z & J & 0 \\ \frac{iDJ'\gamma_3}{2J} & \frac{iDJ'\gamma_2}{2J} & 0 & 0 & 0 & J \end{pmatrix} \begin{pmatrix} \tilde{t}_{x,B,\mathbf{k}} \\ \tilde{t}_{y,B,\mathbf{k}} \\ \tilde{t}_{z,B,\mathbf{k}} \\ \tilde{t}_{x,A,\mathbf{k}} \\ \tilde{t}_{y,A,\mathbf{k}} \\ \tilde{t}_{z,A,\mathbf{k}} \end{pmatrix}$$

analytical solution:

$$\begin{aligned} \omega_{1,2} &= J - \Omega_\mp \\ \omega_{3,4} &= J \\ \omega_{5,6} &= J + \Omega_\pm \end{aligned}$$

4 dispersive bands

2 flat bands

with

$$\Omega_\pm = \sqrt{(h_z \pm 2D'_\perp\gamma_1)^2 + \frac{D^2 J'^2}{4J^2}(\gamma_2^2 + \gamma_3^2)}$$

full bond-wave theory gives
the same results, linear in D

geometrical factors:

$$\gamma_1 = \cos\frac{k_x}{2}\cos\frac{k_y}{2}$$

$$\gamma_2 = \sin\frac{k_x + k_y}{2}$$

$$\gamma_3 = \sin\frac{k_x - k_y}{2}$$

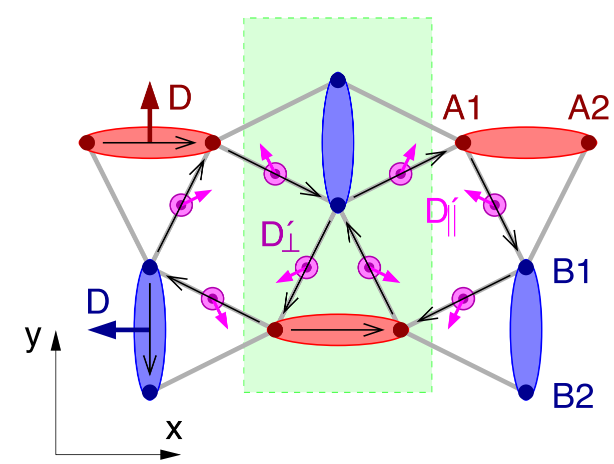

The dispersion:

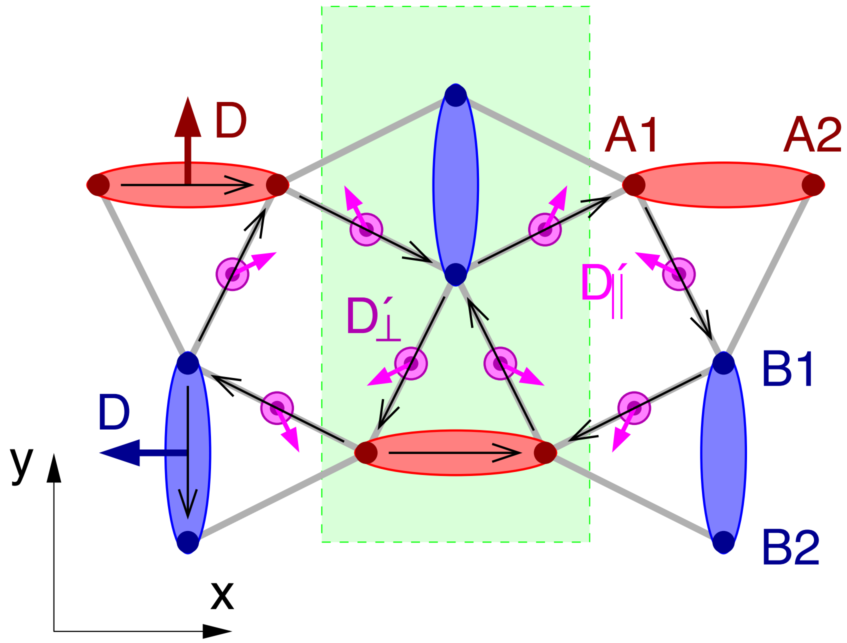

analytical solution:

$$\omega_{1,2} = J - \Omega_{\mp}$$
$$\omega_{3,4} = J$$
$$\omega_{5,6} = J + \Omega_{\pm}$$

4 dispersive bands

2 flat bands

with

$$\Omega_{\pm} = \sqrt{(h_z \pm 2D'_{\perp}\gamma_1)^2 + \frac{D^2 J'^2}{4J^2}(\gamma_2^2 + \gamma_3^2)}$$

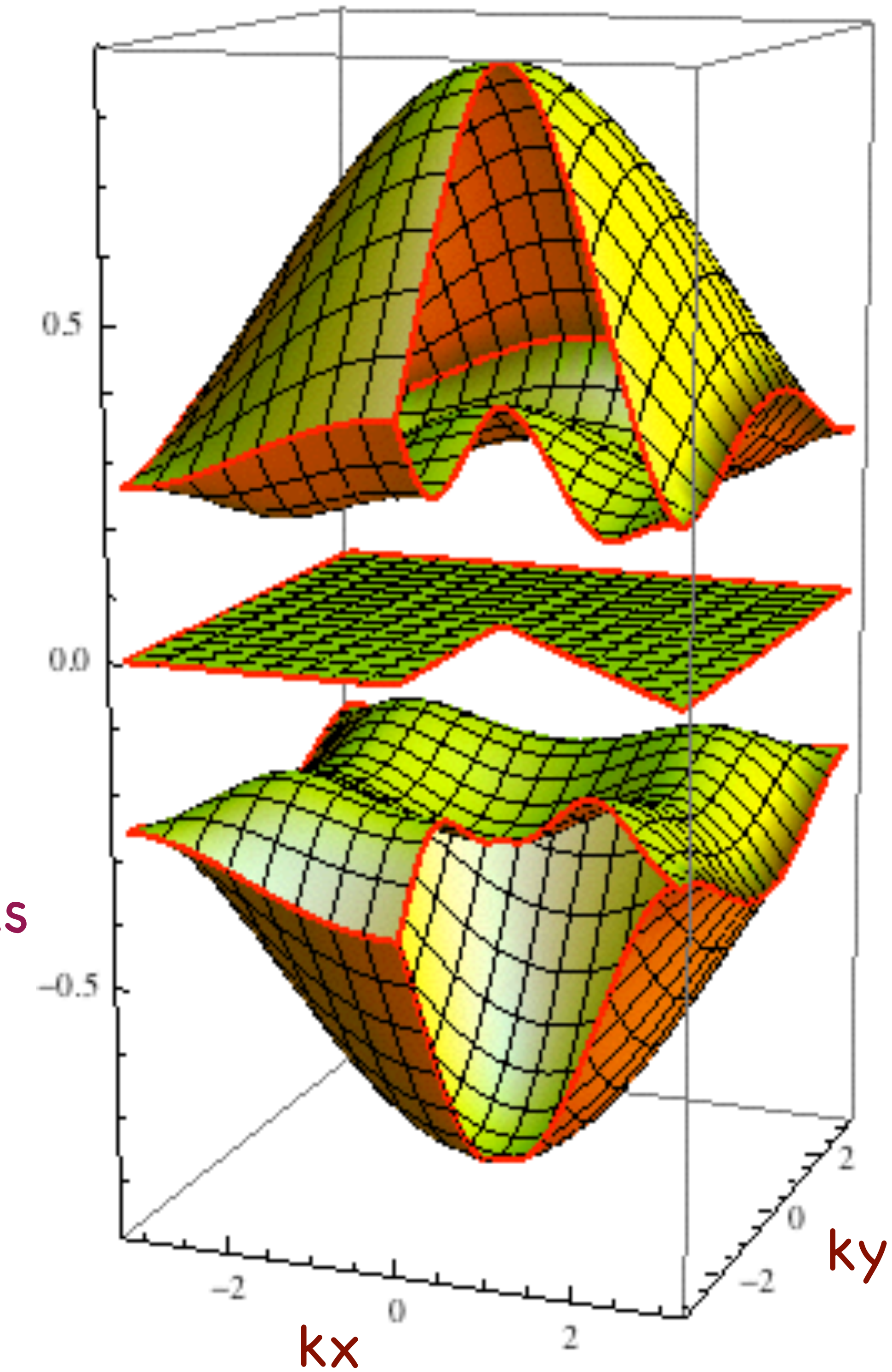

Note: the dispersions are degenerate at the Brillouin zone boundary!

The 3x3 matrix for the triplets

Unfold 6x6 into 3x3

$$\mathcal{H} = \begin{pmatrix} \tilde{t}^{\dagger}_{x,\mathbf{k}} \\ \tilde{t}^{\dagger}_{y,\mathbf{k}} \\ \tilde{t}^{\dagger}_{z,\mathbf{k}} \end{pmatrix}^T \begin{pmatrix} J & ih_z + 2iD'_{\perp}\gamma_1 & -\frac{DJ'}{2J}\gamma_3 \\ -ih_z - 2iD'_{\perp}\gamma_1 & J & -\frac{DJ'}{2J}\gamma_2 \\ -\frac{DJ'}{2J}\gamma_3 & -\frac{DJ'}{2J}\gamma_2 & J \end{pmatrix} \begin{pmatrix} \tilde{t}_{x,\mathbf{k}} \\ \tilde{t}_{y,\mathbf{k}} \\ \tilde{t}_{z,\mathbf{k}} \end{pmatrix}$$

$$\begin{aligned} \tilde{t}_{x,\mathbf{k}} &= \tilde{t}_{x,A,\mathbf{k}} \quad \text{or} \quad -i\tilde{t}_{x,B,\mathbf{k}} \\ \tilde{t}_{y,\mathbf{k}} &= \tilde{t}_{y,A,\mathbf{k}} \quad \text{or} \quad -i\tilde{t}_{y,B,\mathbf{k}} \\ \tilde{t}_{z,\mathbf{k}} &= \tilde{t}_{z,A,\mathbf{k}} \quad \text{or} \quad i\tilde{t}_{z,B,\mathbf{k}} \end{aligned}$$

Band touching transition of triplons in magnetic field

$h_c = 2D'_\perp$

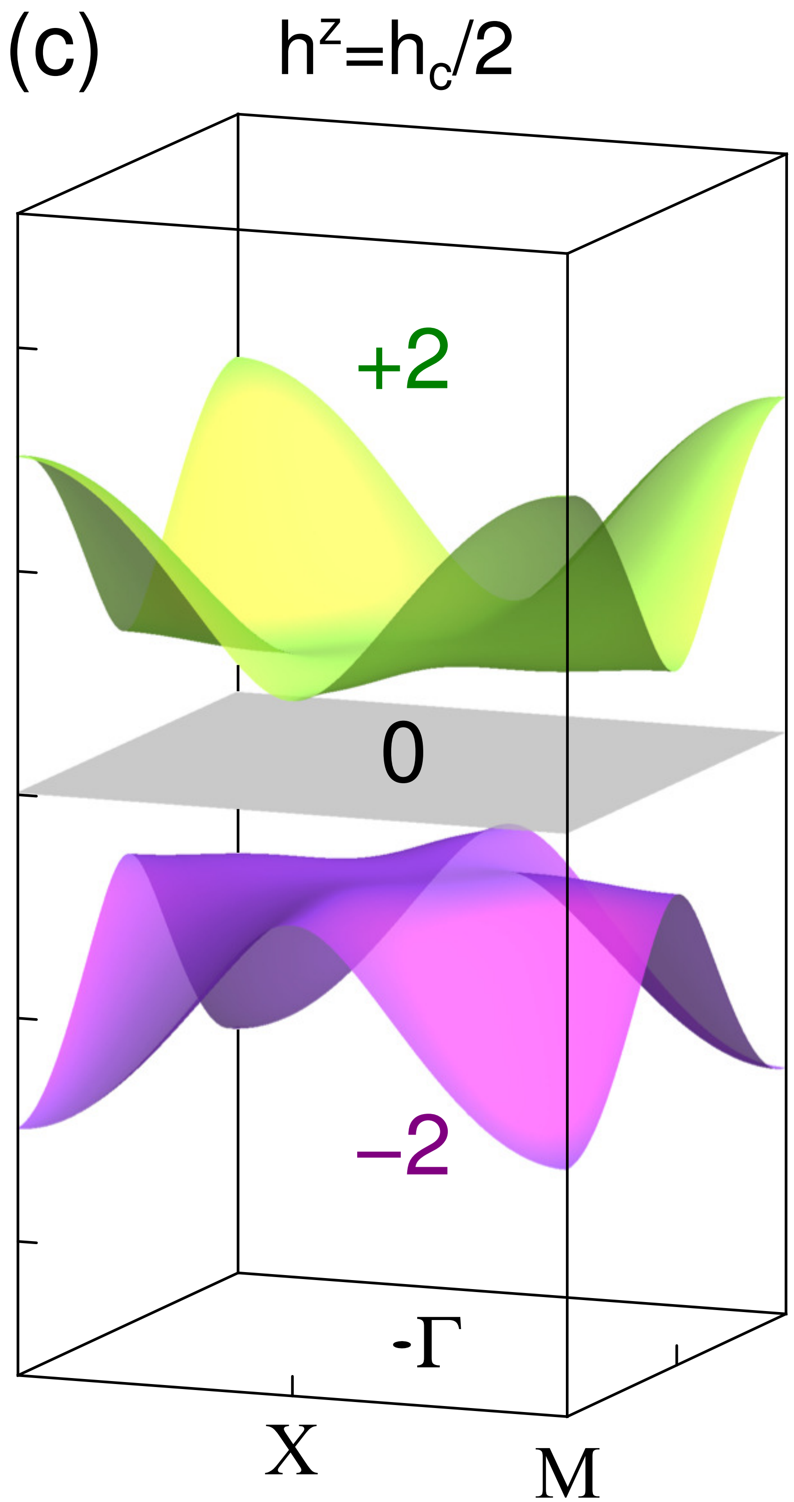

$$C_n = \frac{1}{2\pi i}\int_{BZ} d^2k F_n^{xy}(\mathbf{k}) \; .$$

Berry curvature

$$F_n^{xy}(\mathbf{k}) = \partial_{k_x}\langle n(\mathbf{k})|\partial_{k_y}|n(\mathbf{k})\rangle - \partial_{k_y}\langle n(\mathbf{k})|\partial_{k_x}|n(\mathbf{k})\rangle$$

$|n(\mathbf{k})\rangle$ is the normalized wave function which belongs to $\omega_n(\mathbf{k})$

Band touching transition of triplons in magnetic field

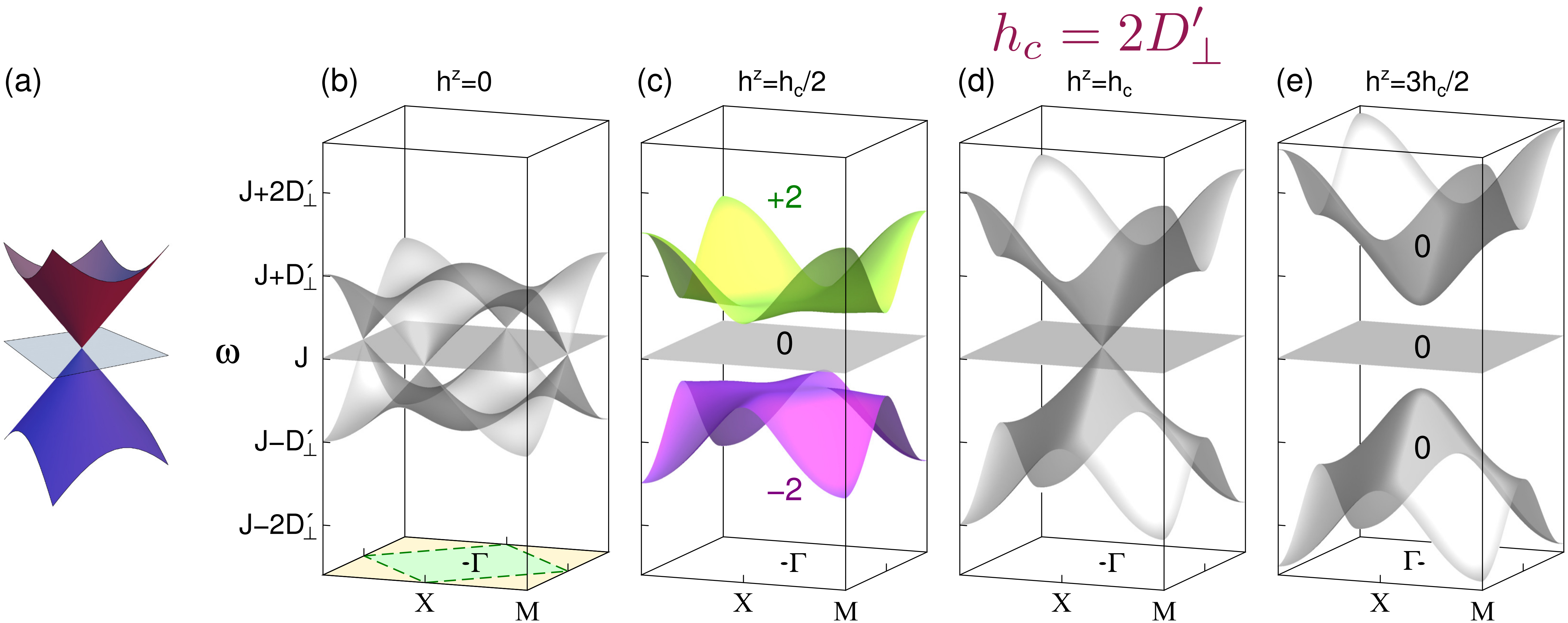

$$C_n = \frac{1}{2\pi i}\int_{BZ} d^2k F_n^{xy}(\mathbf{k}) \ .$$

Berry curvature $F_n^{xy}(\mathbf{k}) = \partial_{k_x}\langle n(\mathbf{k})|\partial_{k_y}|n(\mathbf{k})\rangle - \partial_{k_y}\langle n(\mathbf{k})|\partial_{k_x}|n(\mathbf{k})\rangle$

$|n(\mathbf{k})\rangle$ is the normalized wave function which belongs to $\omega_n(\mathbf{k})$

Band touching transition of triplons in magnetic field

$h_c = 2D'_\perp$

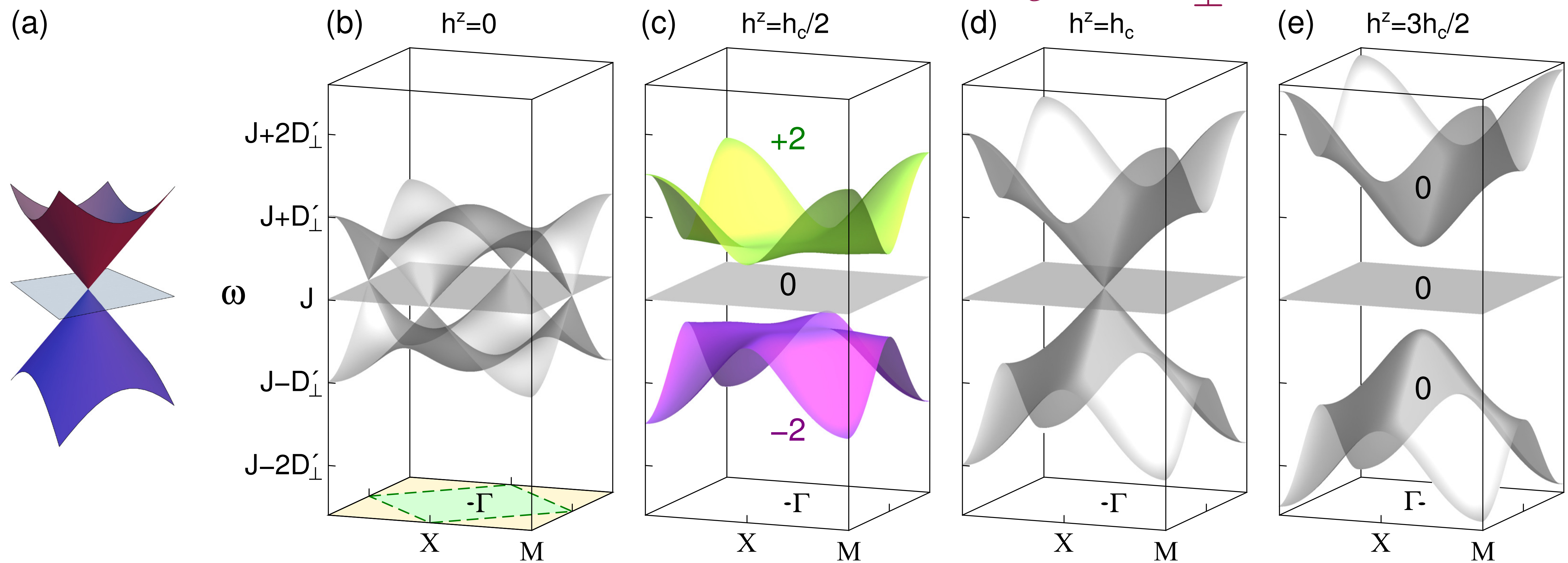

$h = 0$ — topologically nontrivial excitations, finite Chern numbers — $h = h_c$ — topologically trivial

band touching transition

Note: the ground state is trivial all the time!

How do we understand the Chern numbers?

$$\mathcal{H} = \begin{pmatrix} \tilde{t}^{\dagger}_{x,\mathbf{k}} \\ \tilde{t}^{\dagger}_{y,\mathbf{k}} \\ \tilde{t}^{\dagger}_{z,\mathbf{k}} \end{pmatrix}^{T} \begin{pmatrix} J & ih_z + 2iD'_{\perp}\gamma_1 & -\frac{DJ'}{2J}\gamma_3 \\ -ih_z - 2iD'_{\perp}\gamma_1 & J & -\frac{DJ'}{2J}\gamma_2 \\ -\frac{DJ'}{2J}\gamma_3 & -\frac{DJ'}{2J}\gamma_2 & J \end{pmatrix} \begin{pmatrix} \tilde{t}_{x,\mathbf{k}} \\ \tilde{t}_{y,\mathbf{k}} \\ \tilde{t}_{z,\mathbf{k}} \end{pmatrix}$$

How do we understand the Chern numbers?

$$\mathcal{H} = \begin{pmatrix} \tilde{t}^\dagger_{x,\mathbf{k}} \\ \tilde{t}^\dagger_{y,\mathbf{k}} \\ \tilde{t}^\dagger_{z,\mathbf{k}} \end{pmatrix}^T \begin{pmatrix} J & ih_z + 2iD'_\perp\gamma_1 & -\frac{DJ'}{2J}\gamma_3 \\ -ih_z - 2iD'_\perp\gamma_1 & J & -\frac{DJ'}{2J}\gamma_2 \\ -\frac{DJ'}{2J}\gamma_3 & -\frac{DJ'}{2J}\gamma_2 & J \end{pmatrix} \begin{pmatrix} \tilde{t}_{x,\mathbf{k}} \\ \tilde{t}_{y,\mathbf{k}} \\ \tilde{t}_{z,\mathbf{k}} \end{pmatrix}$$

$$Q^x = \begin{pmatrix} 0 & 0 & 1 \\ 0 & 0 & 0 \\ 1 & 0 & 0 \end{pmatrix}$$

$$Q^y = \begin{pmatrix} 0 & 0 & 0 \\ 0 & 0 & 1 \\ 0 & 1 & 0 \end{pmatrix}$$

$$Q^z = \begin{pmatrix} 0 & -i & 0 \\ i & 0 & 0 \\ 0 & 0 & 0 \end{pmatrix}$$

$$[Q^\alpha, Q^\beta] = i\varepsilon_{\alpha\beta\gamma}Q^\gamma$$

Q : generators of an SU(2) algebra, T=1 pseudospin

A more appealing form:

$$H(\mathbf{k}) = J\mathbf{1} - \mathbf{d}(\mathbf{k})\cdot\mathbf{Q}$$

$$\mathbf{d}(\mathbf{k}) = \begin{pmatrix} \frac{DJ'}{2J}\sin\frac{kx-ky}{2} \\ \frac{DJ'}{2J}\sin\frac{kx+ky}{2} \\ h_z + 2D'_\perp\cos\frac{kx}{2}\cos\frac{ky}{2} \end{pmatrix}$$

d(k) : a fictitious magnetic field, Zeeman splits the T=1 pseudospins

Chern number and skyrmions

$$H(\mathbf{k}) = J\mathbf{1} - \mathbf{d}(\mathbf{k})\cdot\mathbf{Q}$$

$$\mathbf{d}(\mathbf{k}) = \begin{pmatrix} \frac{DJ'}{2J}\sin\frac{kx-ky}{2} \\ \frac{DJ'}{2J}\sin\frac{kx+ky}{2} \\ h_z + 2D'_\perp\cos\frac{kx}{2}\cos\frac{ky}{2} \end{pmatrix}$$

Texture of the **d(k)** fictitious magnetic field in the Brillouin zone.
It makes a skyrmion.

$$N_s = \frac{1}{4\pi}\int dk_x dk_y \hat{d}\cdot\left(\partial_y\hat{d}\times\partial_x\hat{d}\right)$$

Chern numbers

C=2

C=0

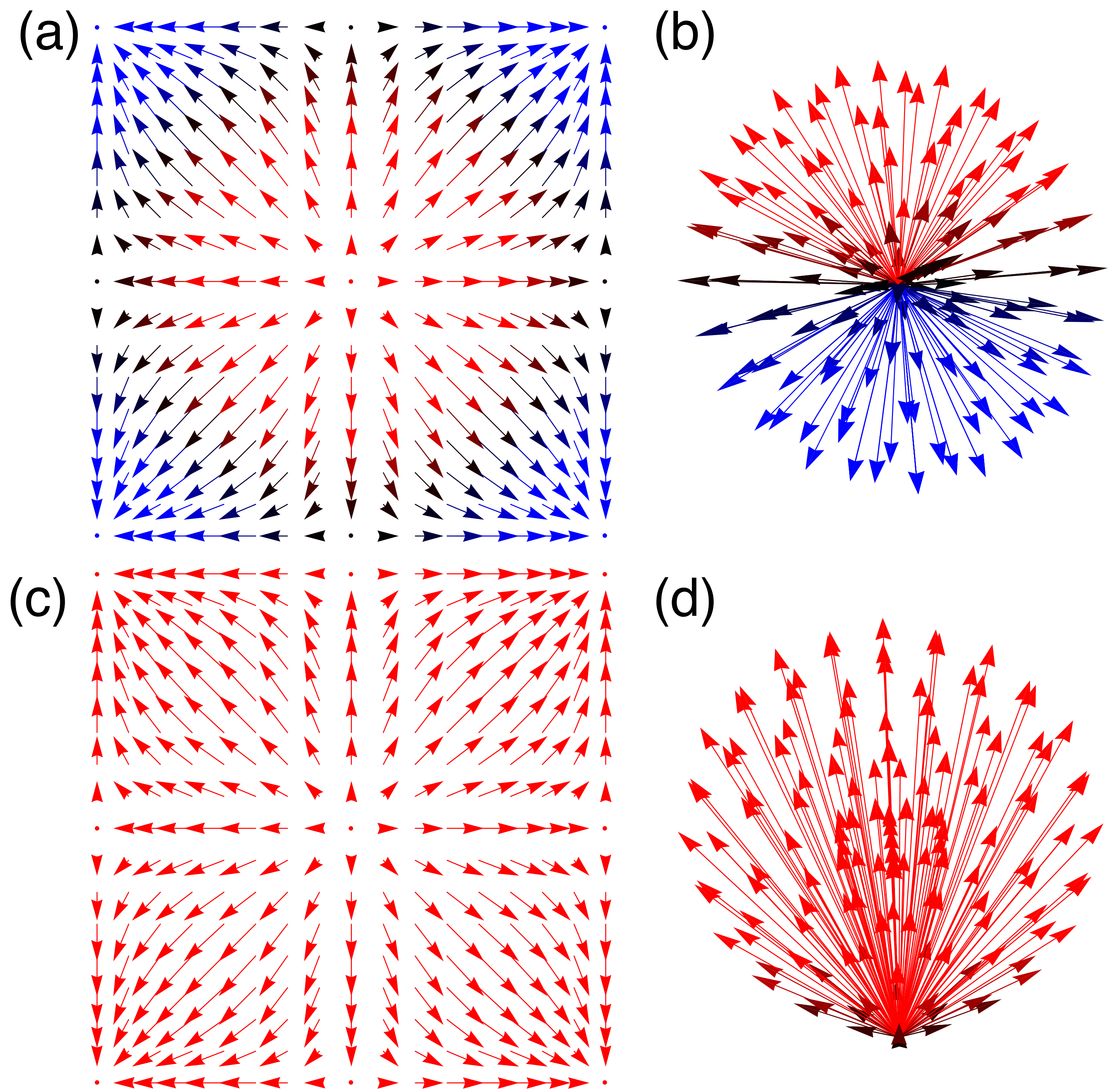

Skyrmion numbers

Ns=1

Ns=0

Band touching and skyrmions

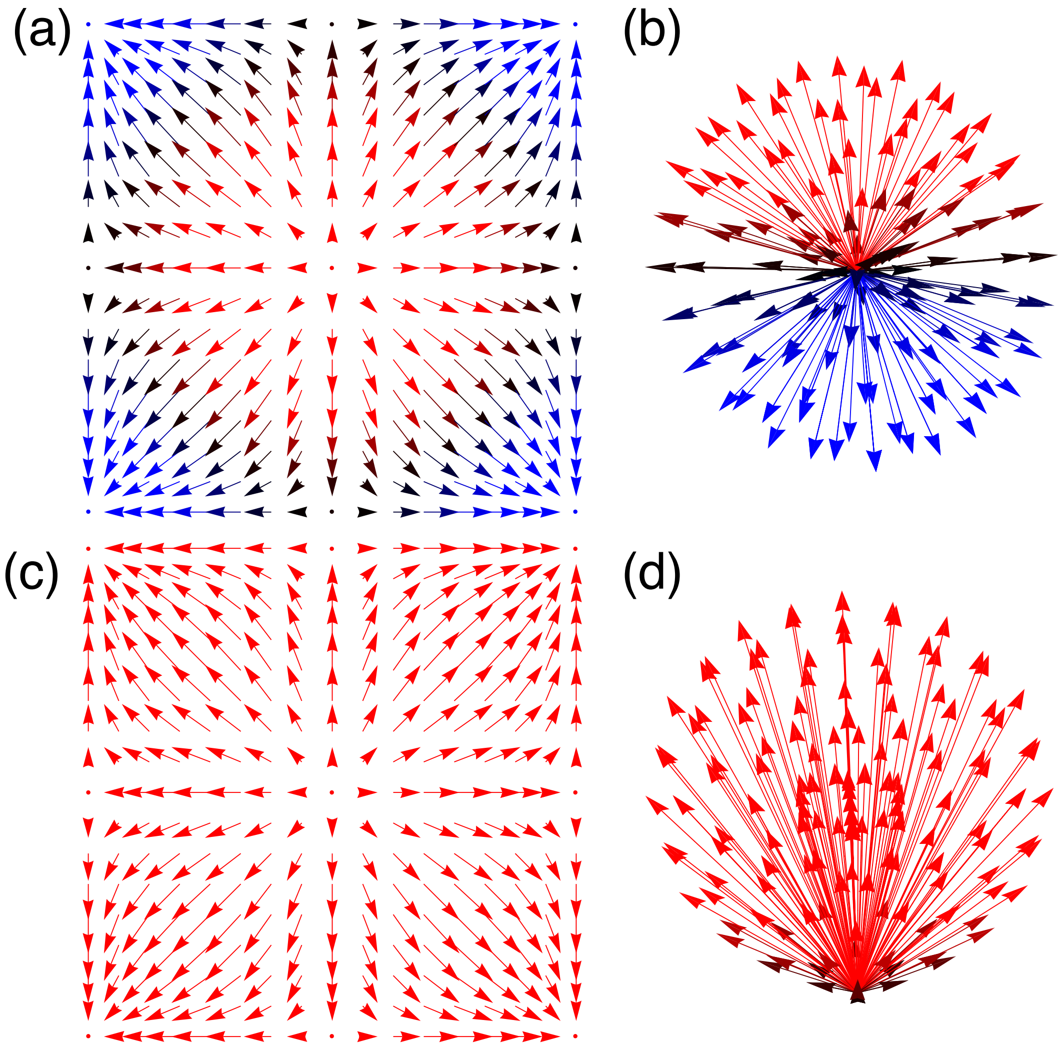

the 2d surface of the **d(k)**

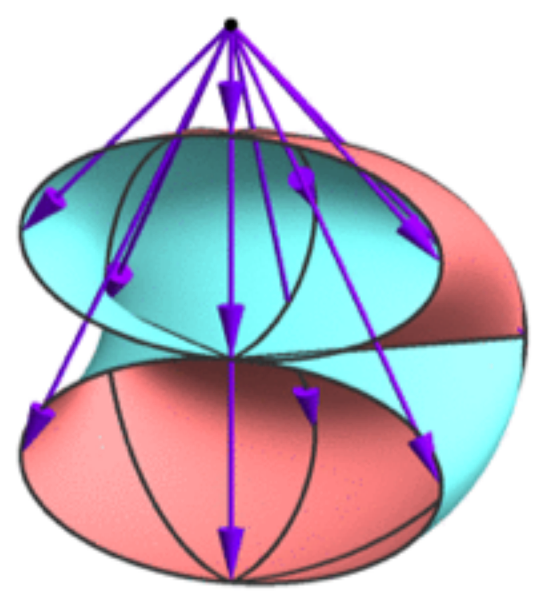

energy dispersion

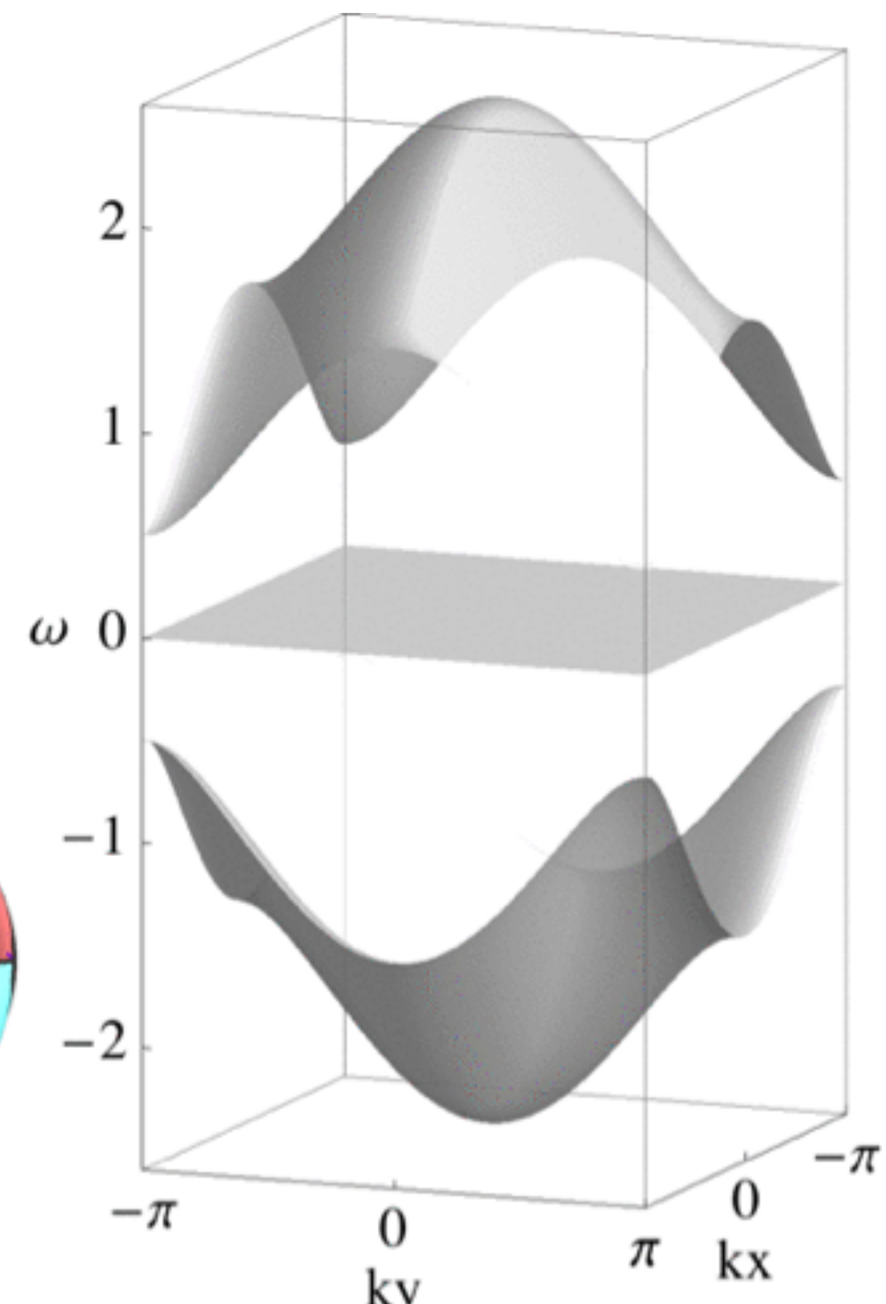

$$\mathbf{d}(\mathbf{k}) = \begin{pmatrix} \frac{DJ'}{2J} \sin \frac{kx-ky}{2} \\ \frac{DJ'}{2J} \sin \frac{kx+ky}{2} \\ h_z + 2D'_\perp \cos \frac{kx}{2} \cos \frac{ky}{2} \end{pmatrix}$$

$$\mathcal{H}(\mathbf{k}) = \mathbf{d}(\mathbf{k}) \cdot \mathbf{Q}$$

Chern number and skyrmions : arbitrary spin

Berry curvature

$$F_n^{xy}(\mathbf{k}) = \partial_x \langle n(\mathbf{k})|\partial_y|n(\mathbf{k})\rangle - \partial_y \langle n(\mathbf{k})|\partial_x|n(\mathbf{k})\rangle$$
$$= 2i \sum_{m\neq n} \mathrm{Im} \frac{\langle n|(\partial_x H)|m\rangle\langle m|(\partial_y H)|n\rangle}{(E_n - E_m)^2}.$$

Hamiltonian (Zeeman levels)

$$H(\mathbf{k}) = J\mathbf{1} - \mathbf{d}(\mathbf{k})\cdot\mathbf{Q}$$
$$H(\mathbf{k})|n\rangle = [J - nd(\mathbf{k})]|n\rangle$$
$$[Q^\alpha, Q^\beta] = i\varepsilon_{\alpha\beta\gamma}Q^\gamma$$ SU(2) algebra

$$F_n^{xy}(\mathbf{k}) = 2i \sum_{\alpha,\beta} \frac{\partial_x d^\alpha(\mathbf{k})\partial_y d^\beta(\mathbf{k})}{d^2(\mathbf{k})} \sum_{m\neq n} \mathrm{Im} \frac{\langle n|Q^\alpha|m\rangle\langle m|Q^\beta|n\rangle}{(n-m)^2}$$
$$= 2i \sum_{\alpha,\beta} \frac{\partial_x d^\alpha(\mathbf{k})\partial_y d^\beta(\mathbf{k})}{d^2(\mathbf{k})} \mathrm{Im}\left(\langle n|Q^\alpha|n{+}1\rangle\langle n{+}1|Q^\beta|n\rangle + \langle n|Q^\alpha|n{-}1\rangle\langle n{-}1|Q^\beta|n\rangle\right)$$
$$\vdots$$
$$= in\hat{\mathbf{d}}(\mathbf{k})\cdot\left(\partial_y\hat{\mathbf{d}}(\mathbf{k})\times\partial_x\hat{\mathbf{d}}(\mathbf{k})\right)$$

the Berry curvature is proportional to the skyrmion density

skyrmion number

$$N_s = \frac{1}{4\pi}\int dk_x dk_y \hat{\mathbf{d}}\cdot\left(\partial_y\hat{\mathbf{d}}\times\partial_x\hat{\mathbf{d}}\right)$$

$$C_n = \frac{1}{2\pi i}\int dk_x dk_y F_n^{xy} = -2nN_s$$

The Chern number of the n-th band is 2n times the number of skyrmions -> 2n edge states

Band touching and Berry curvature

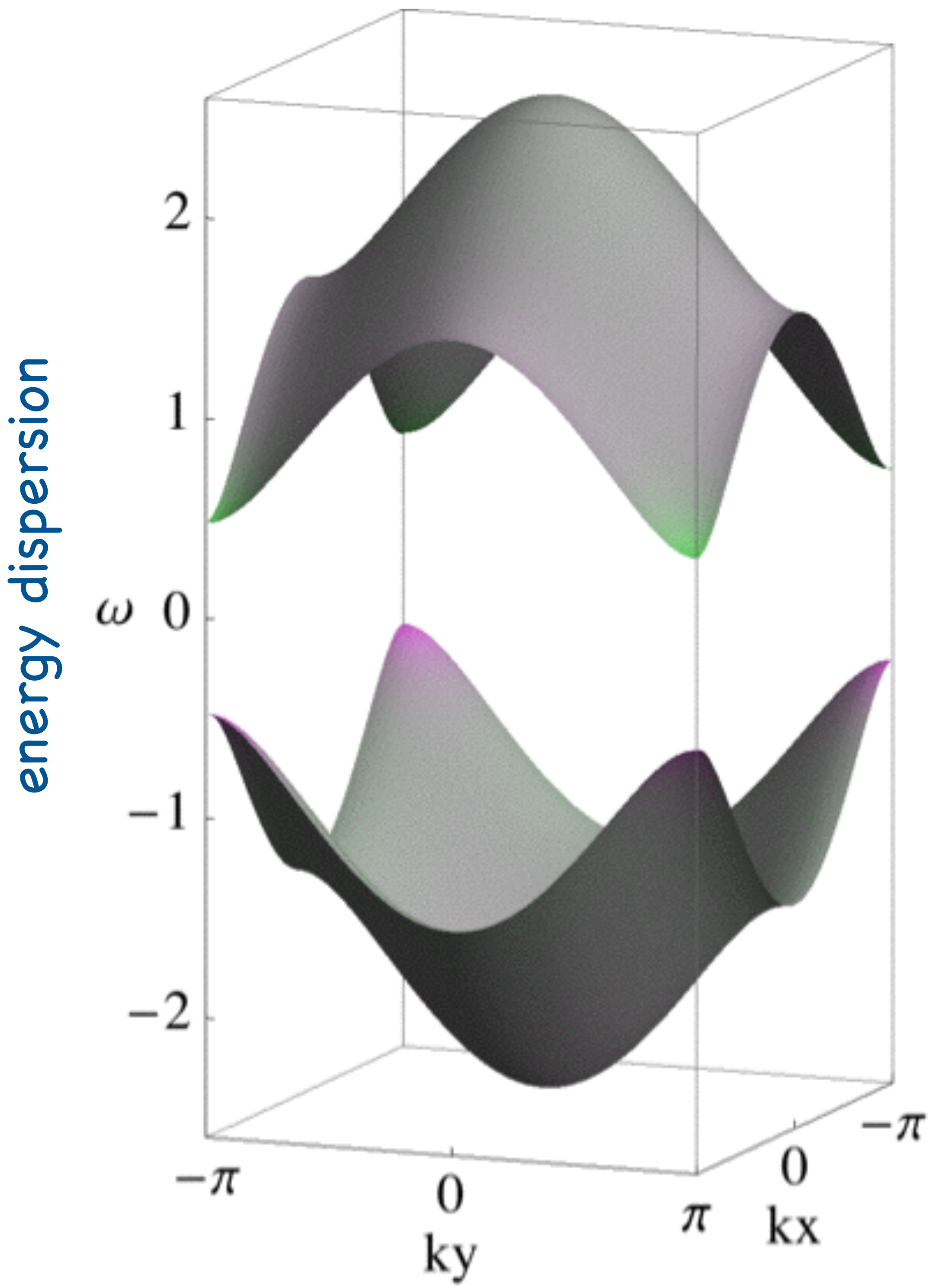

Berry curvature color coded on the energy surface

$$F_n^{xy}(\mathbf{k}) = 2i \sum_{m \neq n} \mathrm{Im} \frac{\langle n|(\partial_x H)|m\rangle \langle m|(\partial_y H)|n\rangle}{(E_n - E_m)^2}.$$

$$\mathcal{H}(\mathbf{k}) = \mathbf{d}(\mathbf{k}) \cdot \mathbf{Q}$$

$$\mathbf{d}(\mathbf{k}) = \begin{pmatrix} \frac{DJ'}{2J} \sin \frac{kx-ky}{2} \\ \frac{DJ'}{2J} \sin \frac{kx+ky}{2} \\ h_z + 2D'_\perp \cos \frac{kx}{2} \cos \frac{ky}{2} \end{pmatrix}$$

Band touching transition in magnetic field vs ESR

triplon density of states

the blue and red lines are at the Γ point

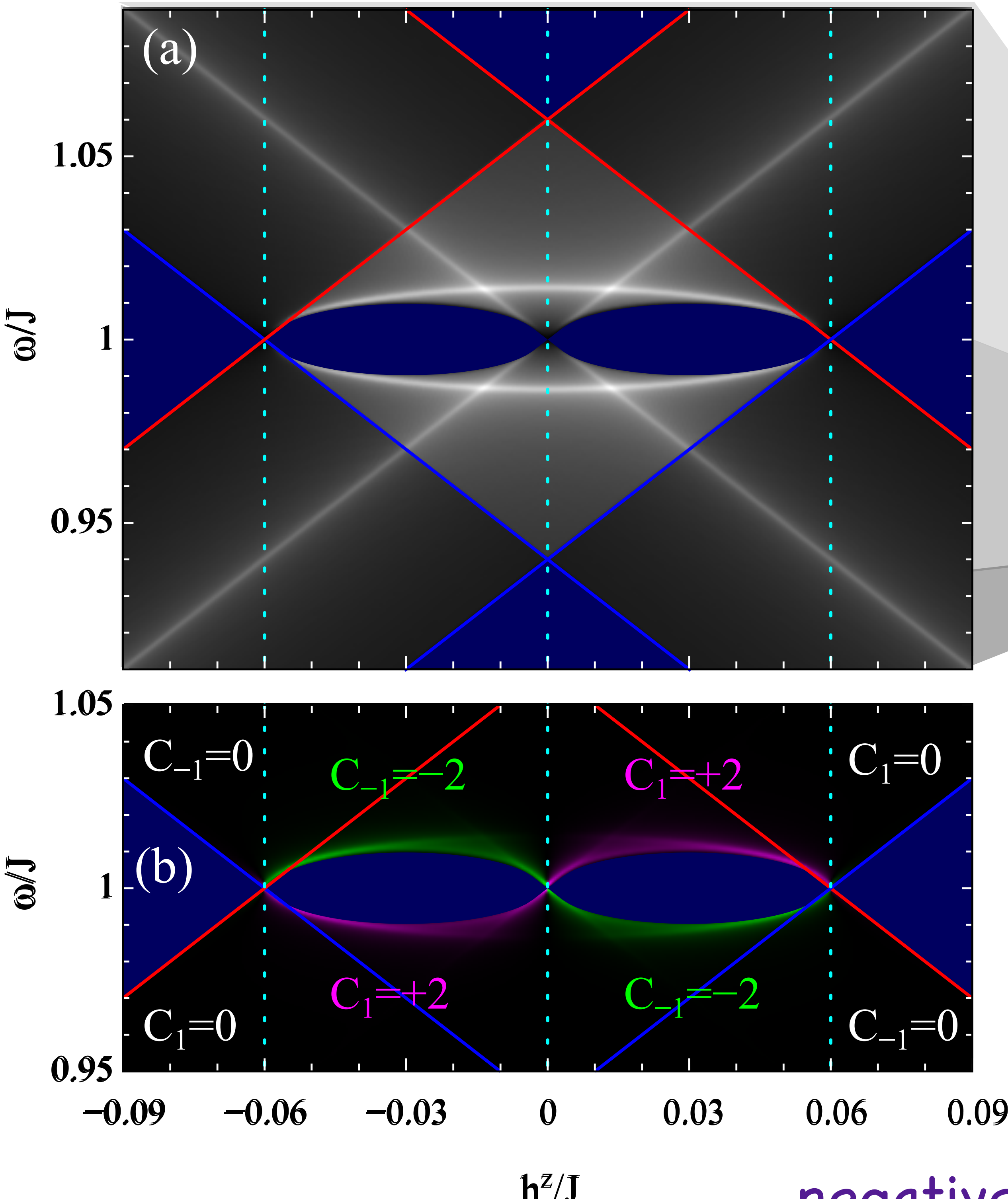

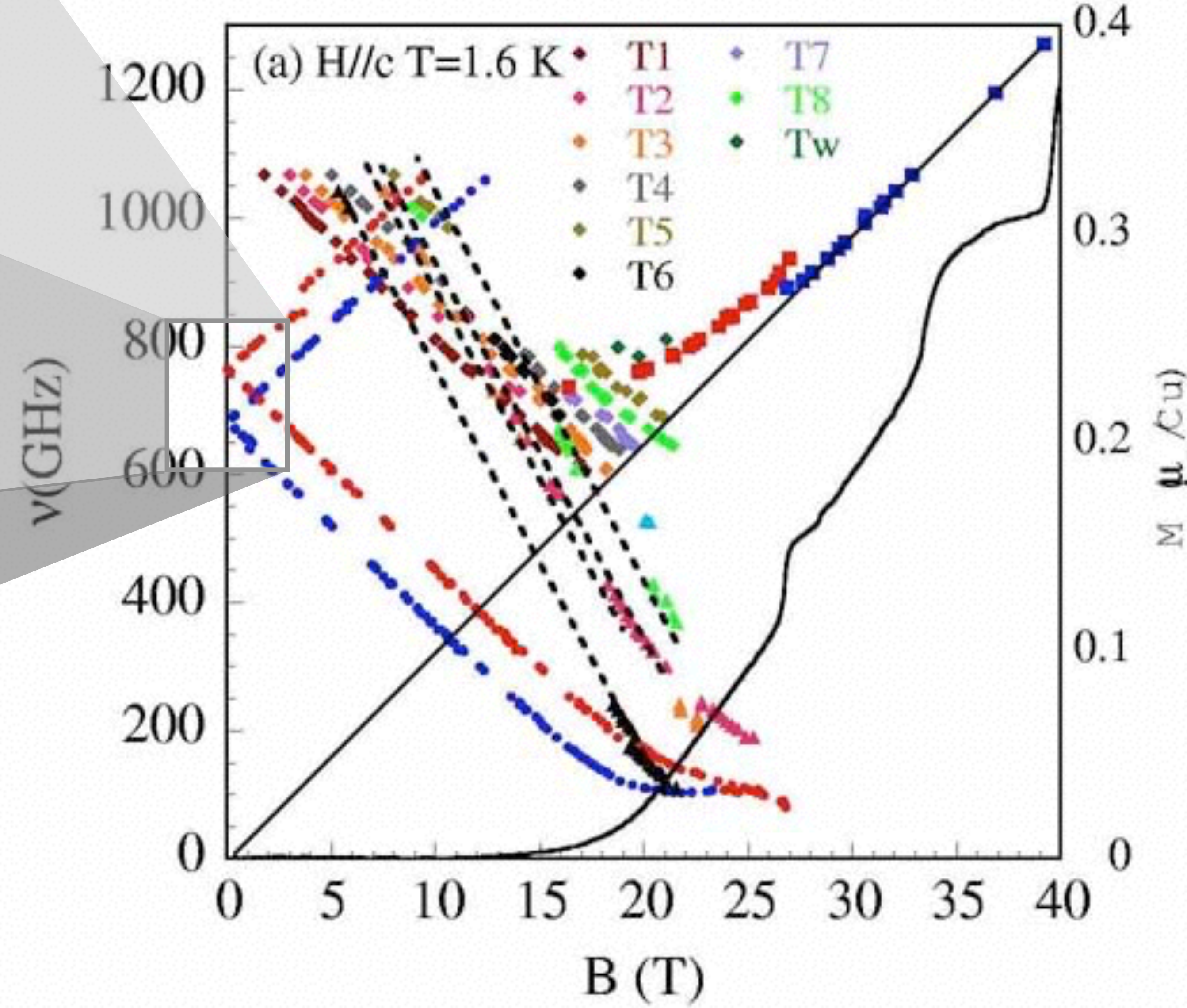

negative/positive

Berry curvature

Band touching transition in magnetic field vs ESR

A Dirac cone in the neutron inelastic spectrum at h_c:

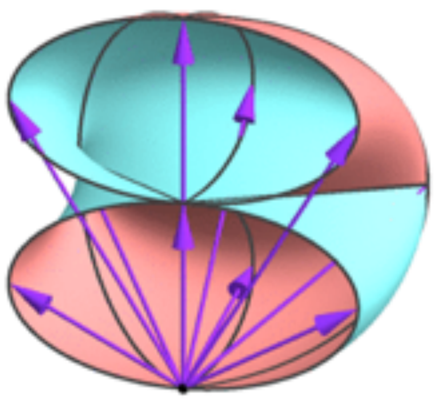

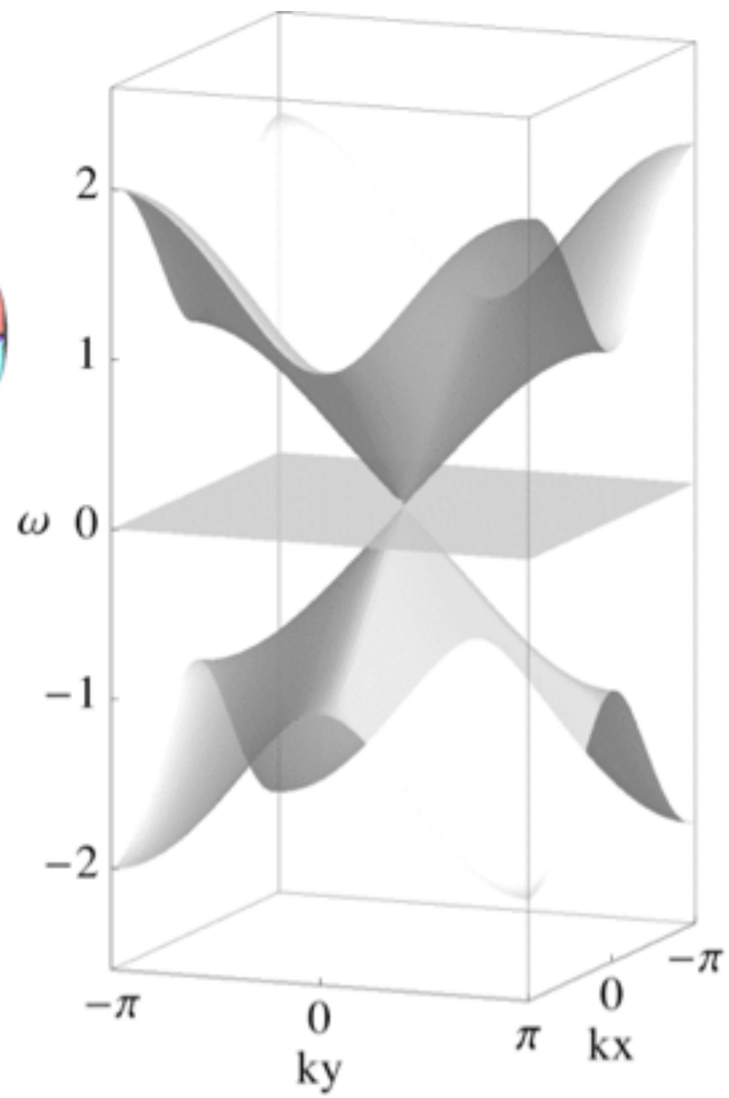

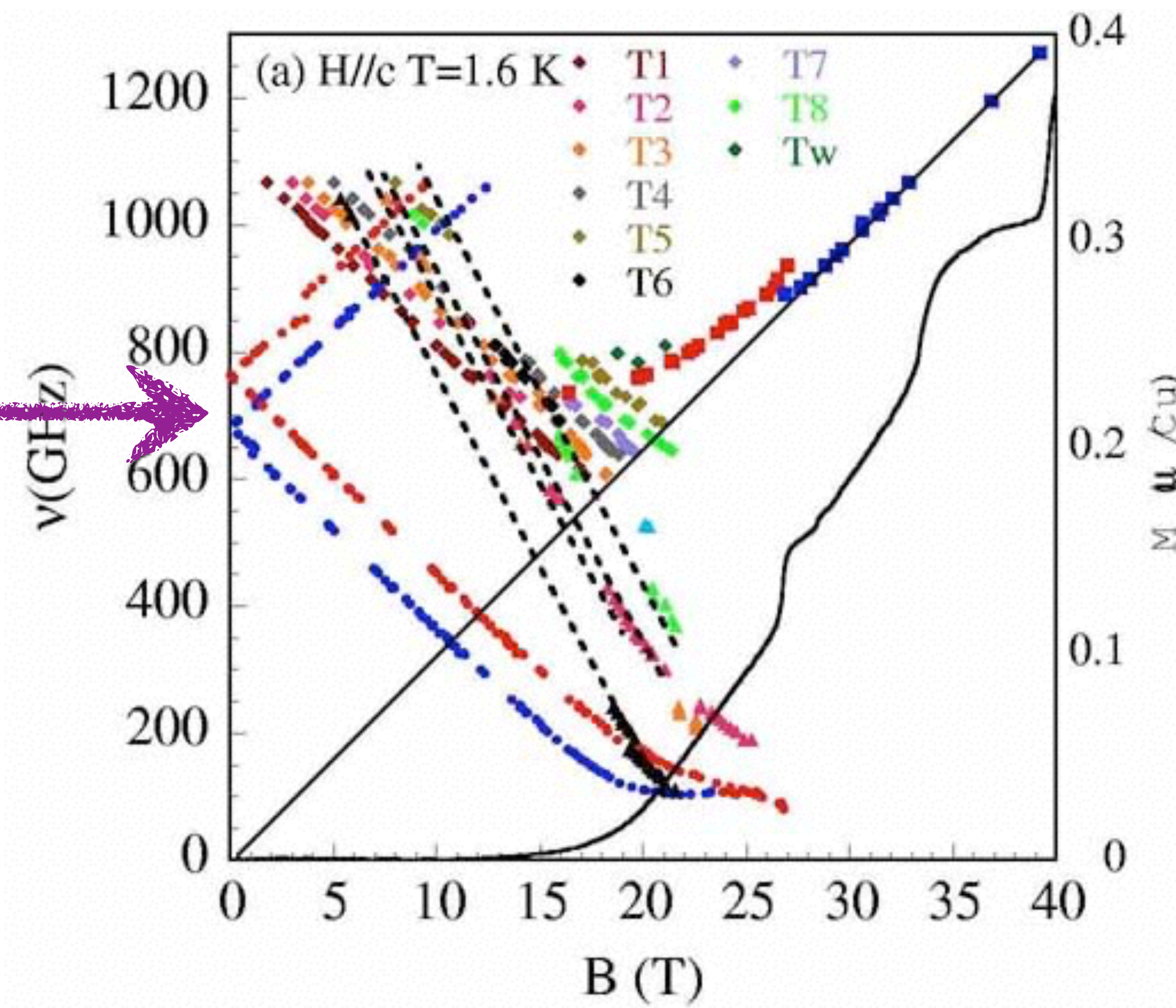

$$h_c = 2D'_\perp$$

Edge states and local density of triplons

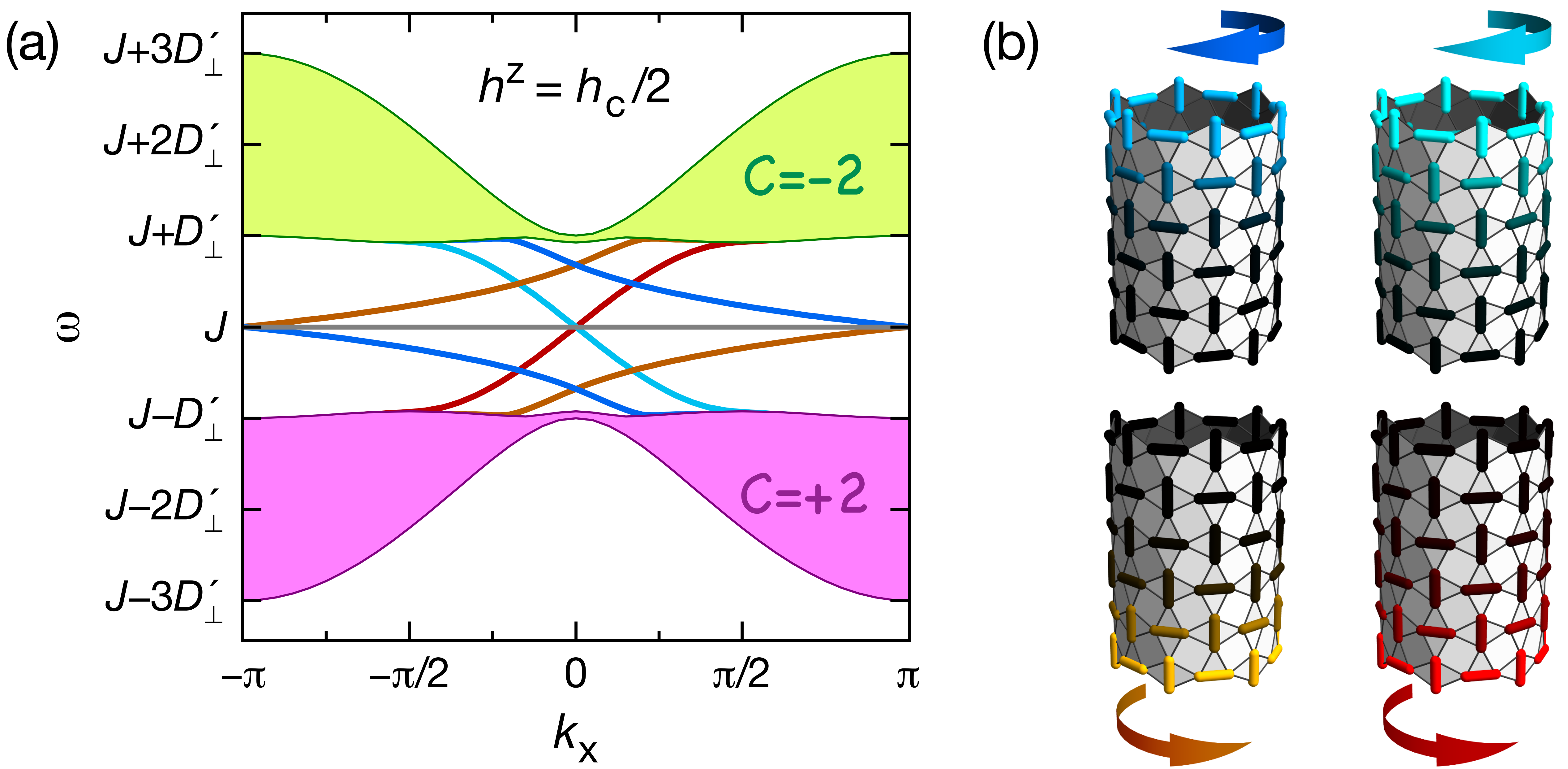

number of edge states is given by C Chern numbers

edge state carry energy and spin current

Thermal Hall Conductivity

Chern bands in electrons $\longrightarrow$ quantum Hall effect

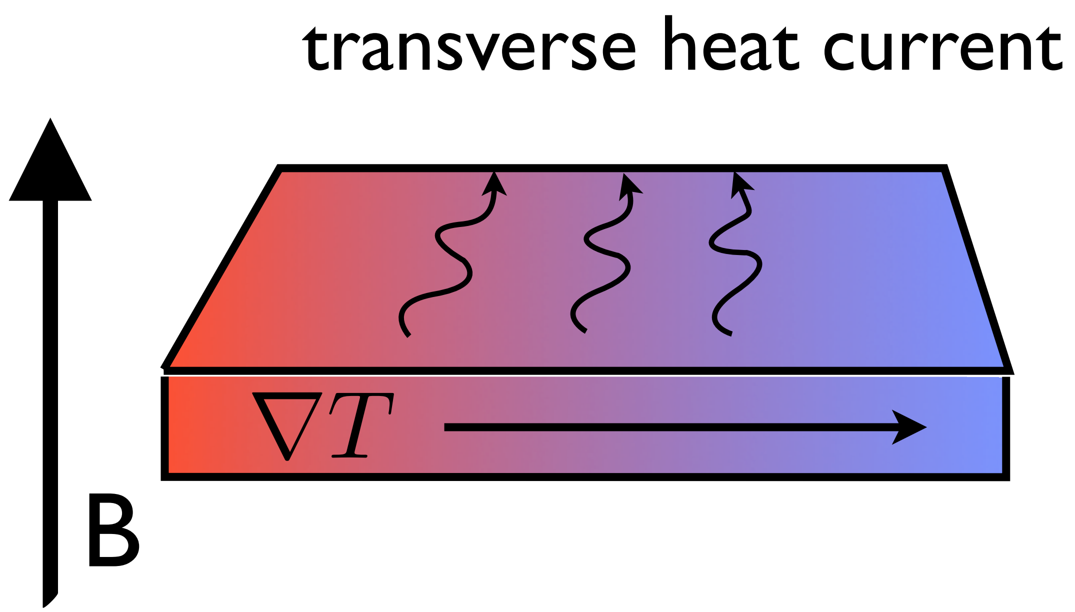

$$\kappa^{xy} = \frac{1}{\beta} \sum_n \int_{\mathrm{BZ}} d^2\mathbf{k}\; c_2(\rho_n) \frac{F_n^{xy}(\mathbf{k})}{i}$$

$$\rho_n = \frac{1}{e^{\omega_n \beta} - 1}$$

$$c_2(\rho) = \int_0^\rho dt\; \ln^2(1 + t^{-1})$$

thermal Hall effect in bosons: linear response (Kubo formula) formalism

Katsura et al., PRL **104**, 066403 (2010),

Matsumoto et al PRL **106** 197202, (2011)

Observation of the Magnon Hall Effect

SCIENCE VOL 329 16 JULY 2010

Y. Onose,[1,2]* T. Ideue,[1] H. Katsura,[3] Y. Shiomi,[1,4] N. Nagaosa,[1,4] Y. Tokura[1,2,4]

$Lu_2V_2O_7$ is a FM insulator

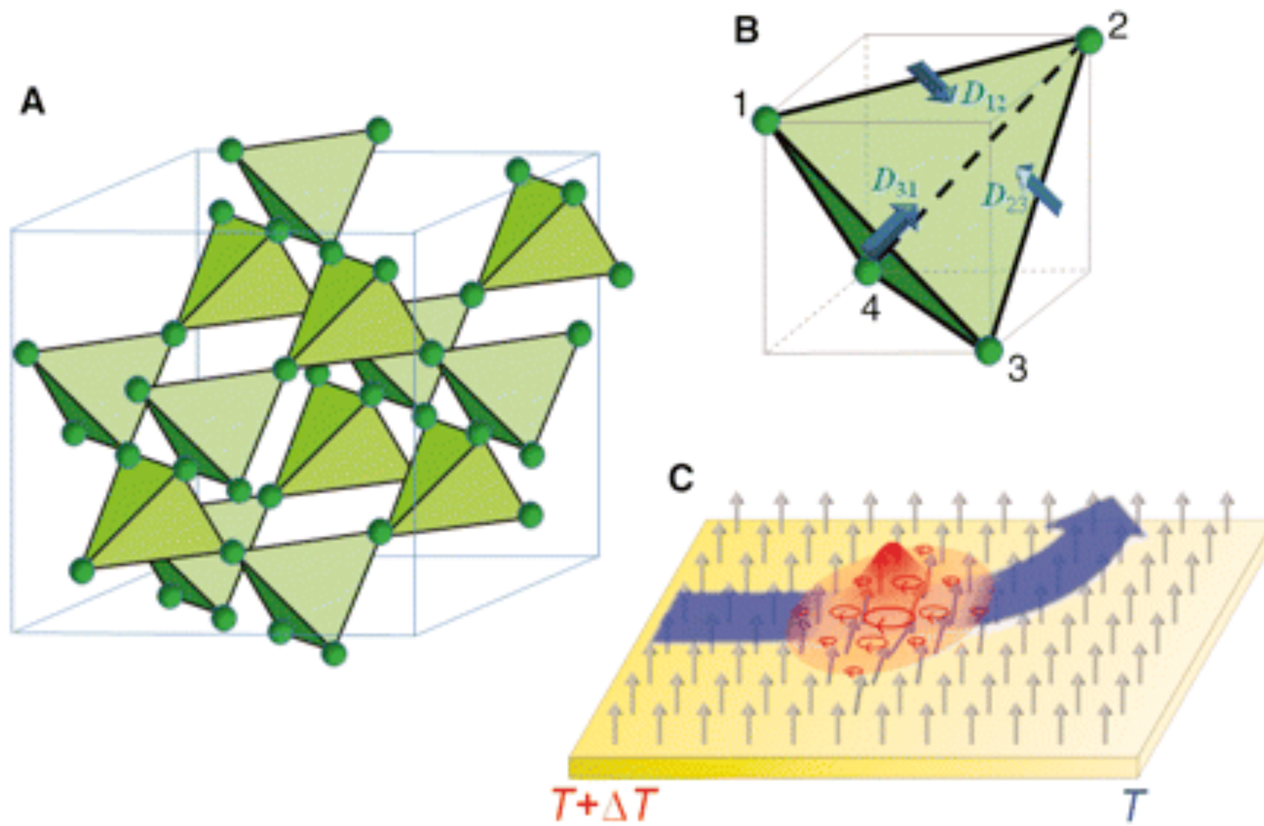

The crystal structure of $Lu_2V_2O_7$ and the magnon Hall effect. (**A**) The *V* sublattice of $Lu_2V_2O_7$, which is composed of corner-sharing tetrahedra. (**B**) The direction of the Dzyaloshinskii-Moriya vector on each bond of the tetrahedron. The Dzyaloshinskii-Moriya interaction acts between the *i* and *j* sites. (**C**) The magnon Hall effect. A wave packet of magnon (a quantum of spin precession) moving from the hot to the cold side is deflected by the Dzyaloshinskii-Moriya interaction playing the role of a vector potential.

Magnetic field variation of the thermal Hall conductivity of $Lu_2V_2O_7$ at various temperatures. The magnetic field is applied along the [100] direction. The solid lines are guides to the eye.

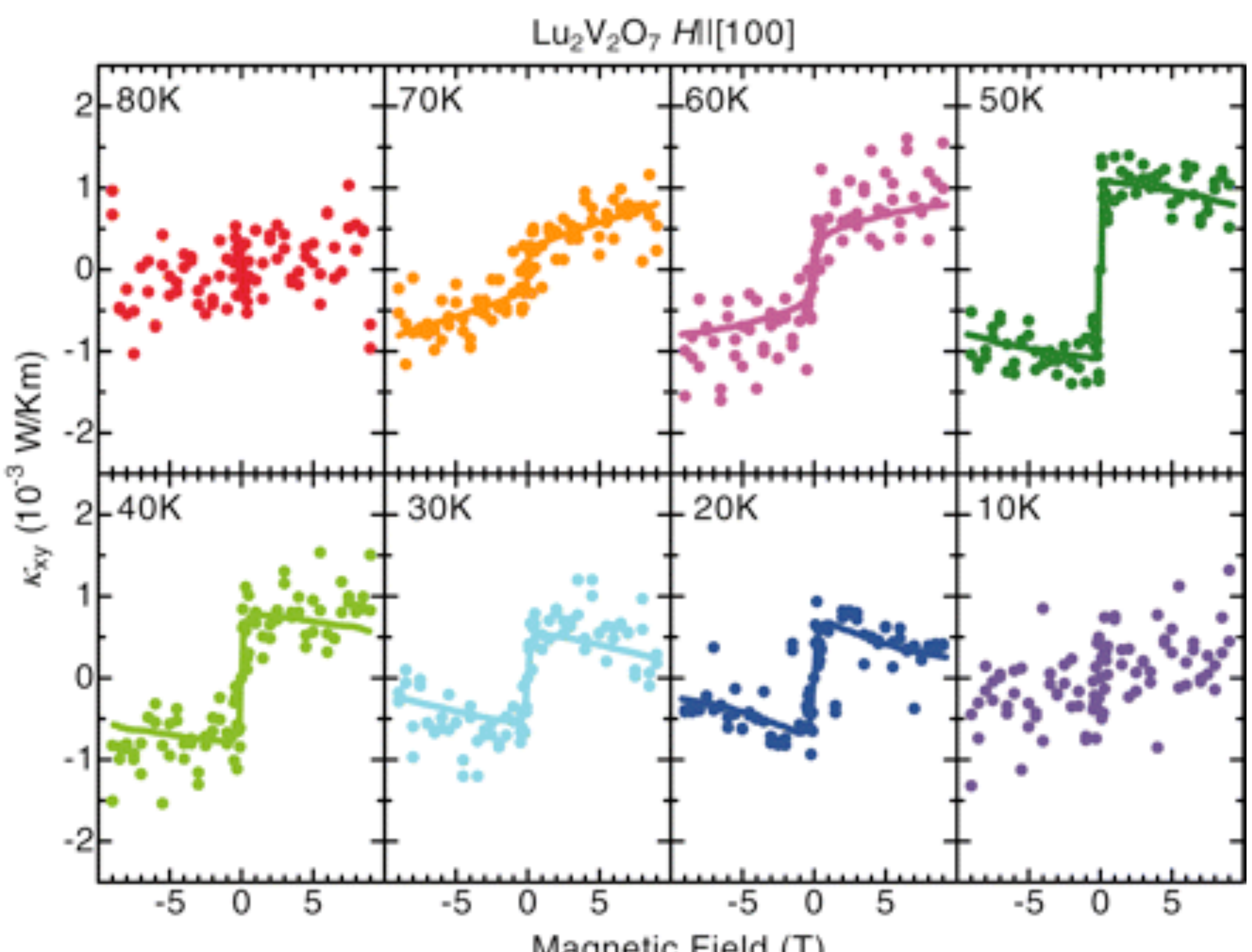

Thermal Hall conductivity in the frustrated pyrochlore magnet $Tb_2Ti_2O_7$

M. Hirschberger, J. W. Krizan,
R. J. Cava, and N. P. Ong

arxiv 1502.02006

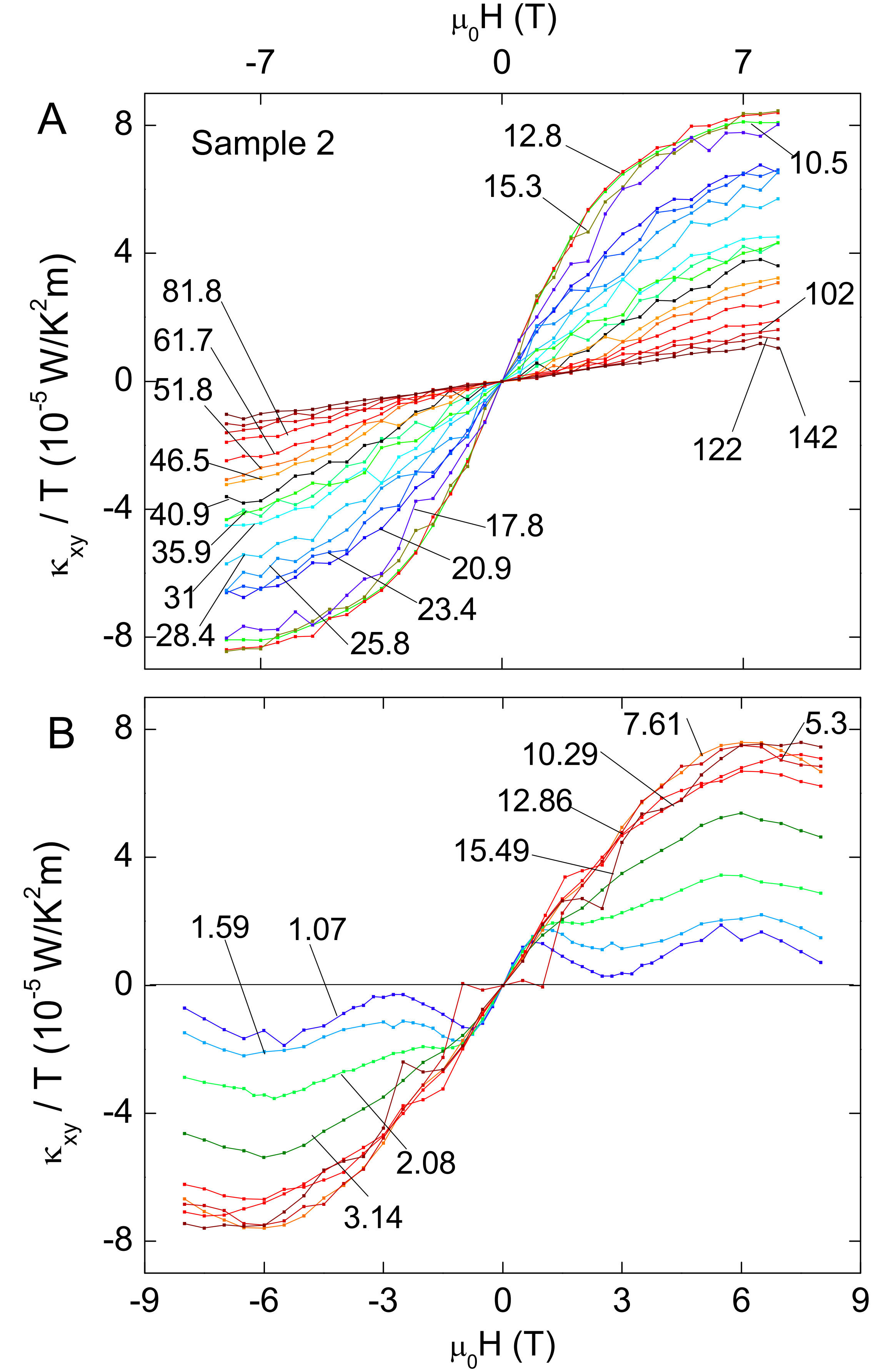

FIG. 3: Curves of the thermal Hall conductivity κ_{xy}/T vs. H in $Tb_2Ti_2O_7$ (Sample 2). From 140 to 50 K, κ_{xy}/T, is H-linear (Panel A). Below 45 K, it develops pronounced curvature at large H, reaching its largest value near 12 K. The sign is always "hole-like". Panel B shows the curves below 15 K. A prominent feature is that the weak-field slope $[\kappa_{xy}/TB]_0$ is nearly T independent below 15 K. Below 3 K, the field profile changes qualitatively, showing additional features that become prominent as T → 0, namely the sharp peak near 1 T and the broad maximum at 6 T.

Thermal Hall Conductivity

Chern bands in electrons → quantum Hall effect

Triplons do not carry charge currents, only heat (energy) current

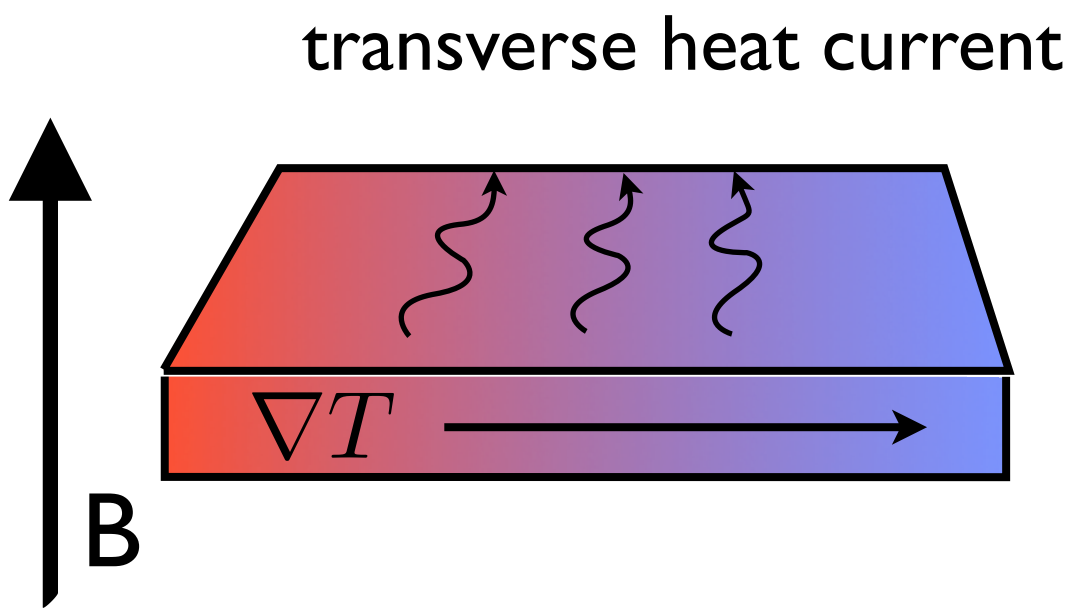

$$\kappa^{xy} = \frac{1}{\beta}\sum_n \int_{\mathrm{BZ}} d^2\mathbf{k}\; c_2(\rho_n)\frac{F_n^{xy}(\mathbf{k})}{i}$$

$$\rho_n = \frac{1}{e^{\omega_n \beta} - 1}$$

$$c_2(\rho) = \int_0^\rho dt\;\ln^2(1 + t^{-1})$$

thermal Hall effect in bosons: linear response (Kubo formula) formalism

Katsura et al., PRL **104**, 066403 (2010),

Matsumoto et al PRL **106** 197202, (2011)

Thermal Hall Conductivity

Chern bands in electrons ⟶ quantum Hall effect

Triplons do not carry charge currents, only heat (energy) current

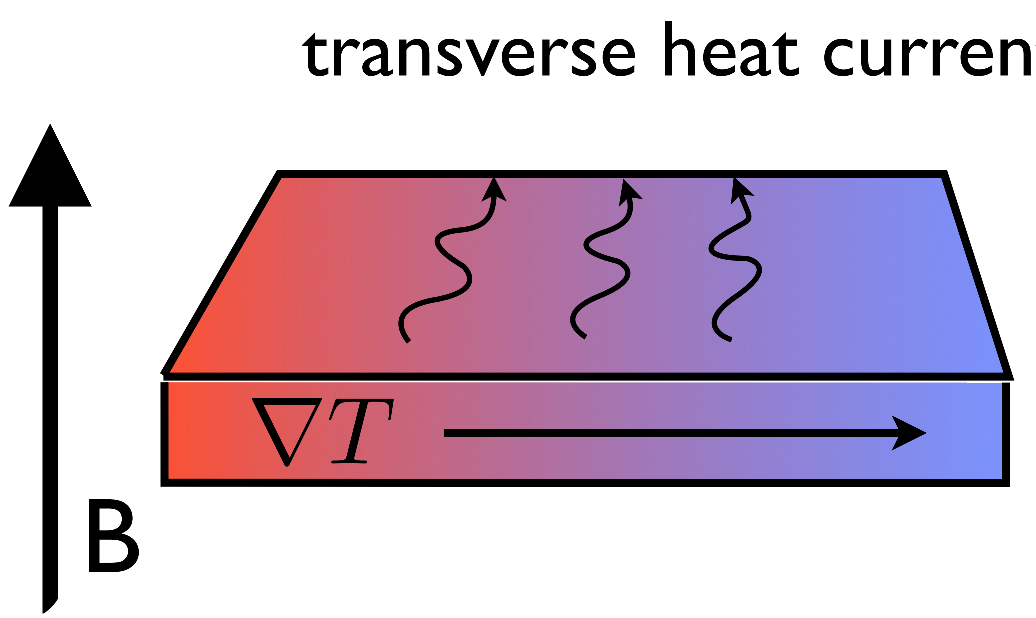

$$\kappa^{xy}(\beta) = R(\omega_0 \beta)\kappa^{xy}_{\infty}$$

$$R(x) = \frac{x^2}{4\sinh^2\frac{x}{2}}$$

$$\kappa^{xy}_{\infty} = \int_{\mathrm{BZ}} d^2\mathbf{k}\,\frac{2}{d^2}\mathbf{d}\cdot\left(\frac{\partial \mathbf{d}}{\partial k_x}\times\frac{\partial \mathbf{d}}{\partial k_y}\right)$$

thermal Hall effect in bosons: linear response (Kubo formula) formalism

Katsura et al., PRL **104**, 066403 (2010),

Matsumoto et al PRL **106** 197202, (2011)

Thermal Hall Conductivity

Chern bands in electrons → quantum Hall effect

Triplons do not carry charge currents, only heat (energy) current

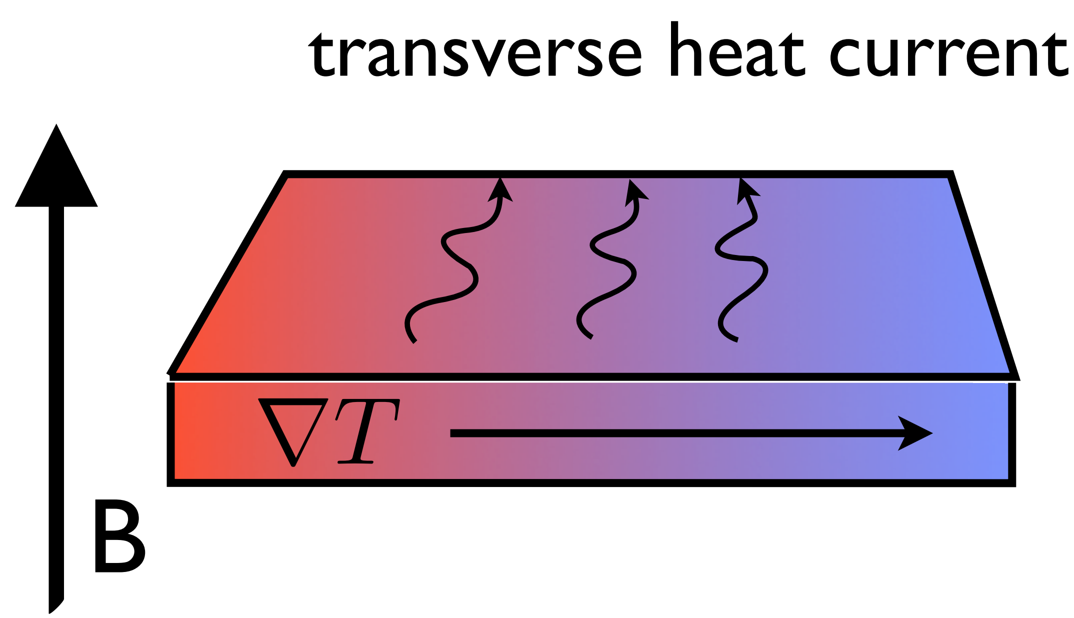

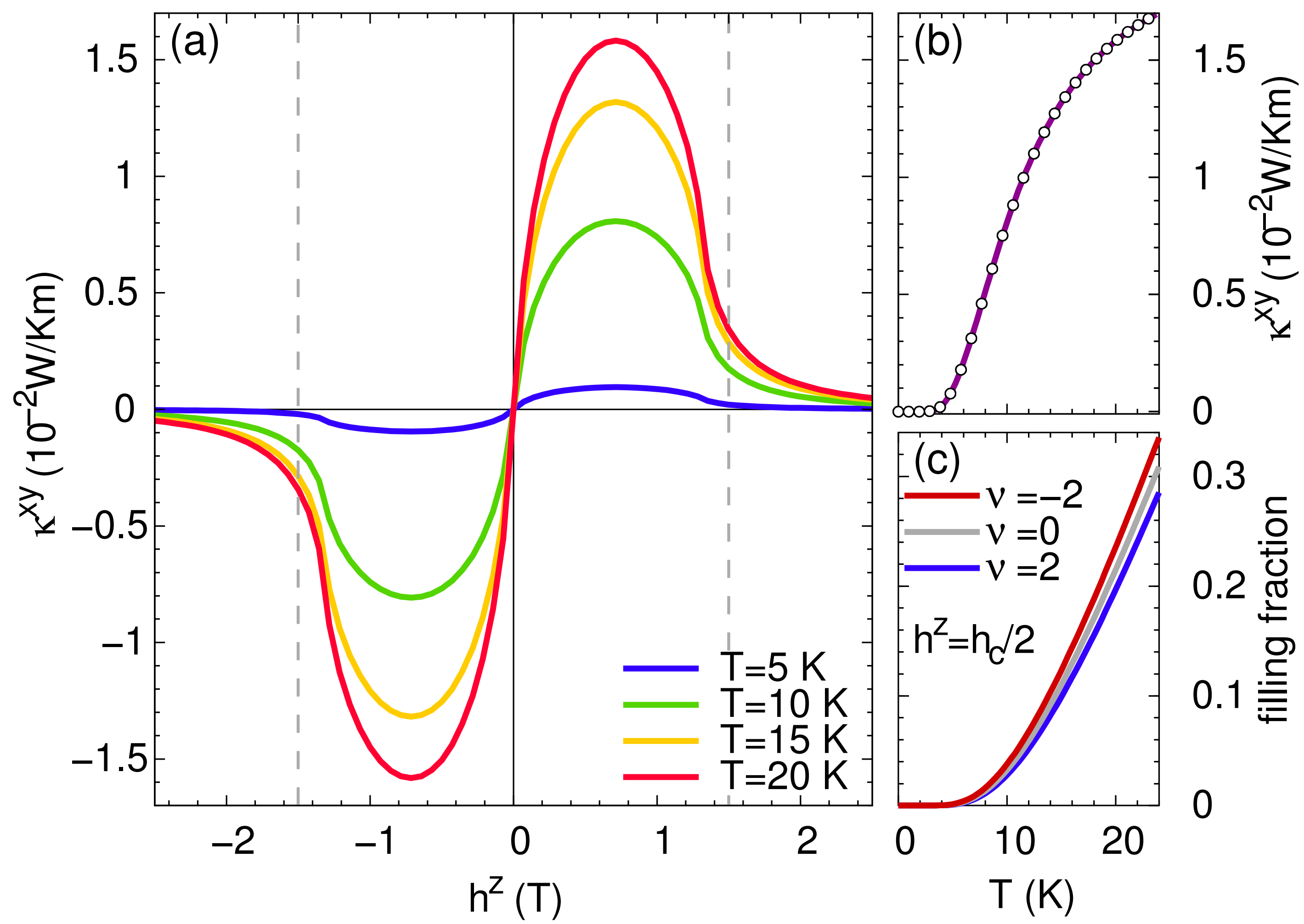

thermal Hall effect in bosons: linear response (Kubo formula) formalism

Katsura et al., PRL **104**, 066403 (2010),

Matsumoto et al PRL **106** 197202, (2011)

effect of diagonal 2nd neighbor hopping

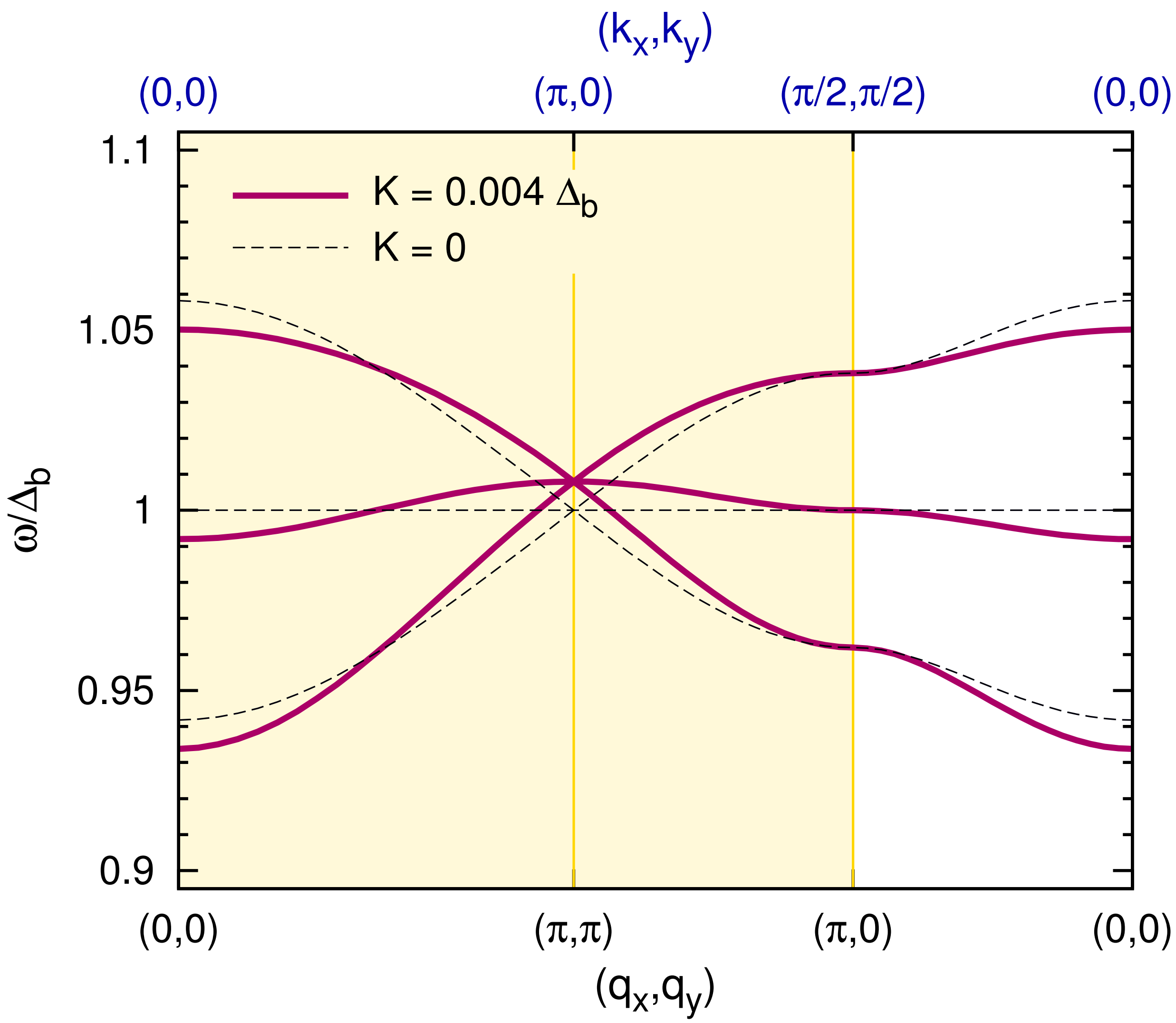

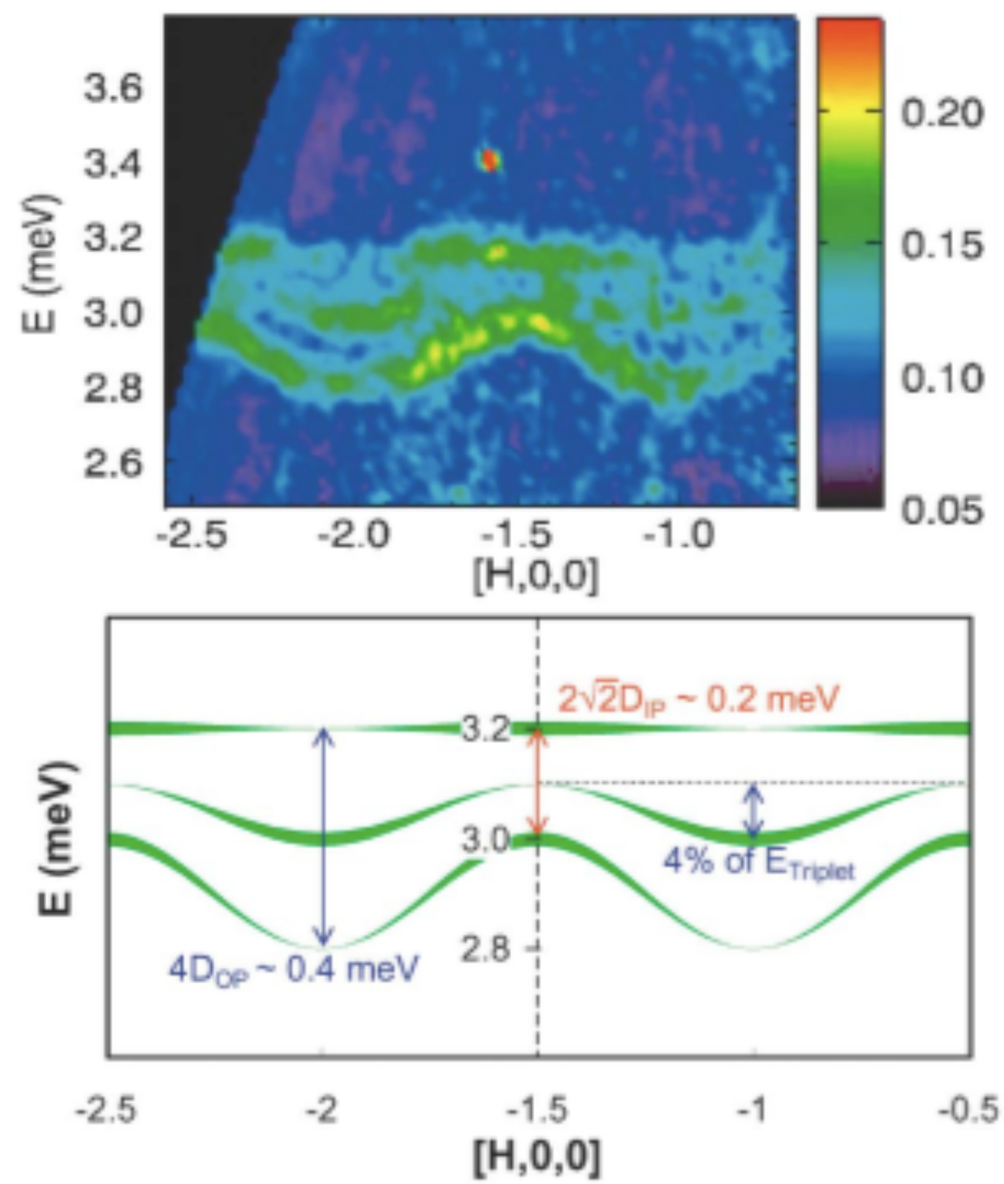

The triplet dispersion due to J′ (6th order process) are missing from our treatment.

B. Gaulin et al., PRL **93**, 267202 (2004)

$$\mathcal{H}(\mathbf{k}) = [J - K_2\gamma_4(\mathbf{k})] + \mathbf{d}(\mathbf{k}) \cdot \mathbf{Q}$$

Effect of second neighbor triplon hopping

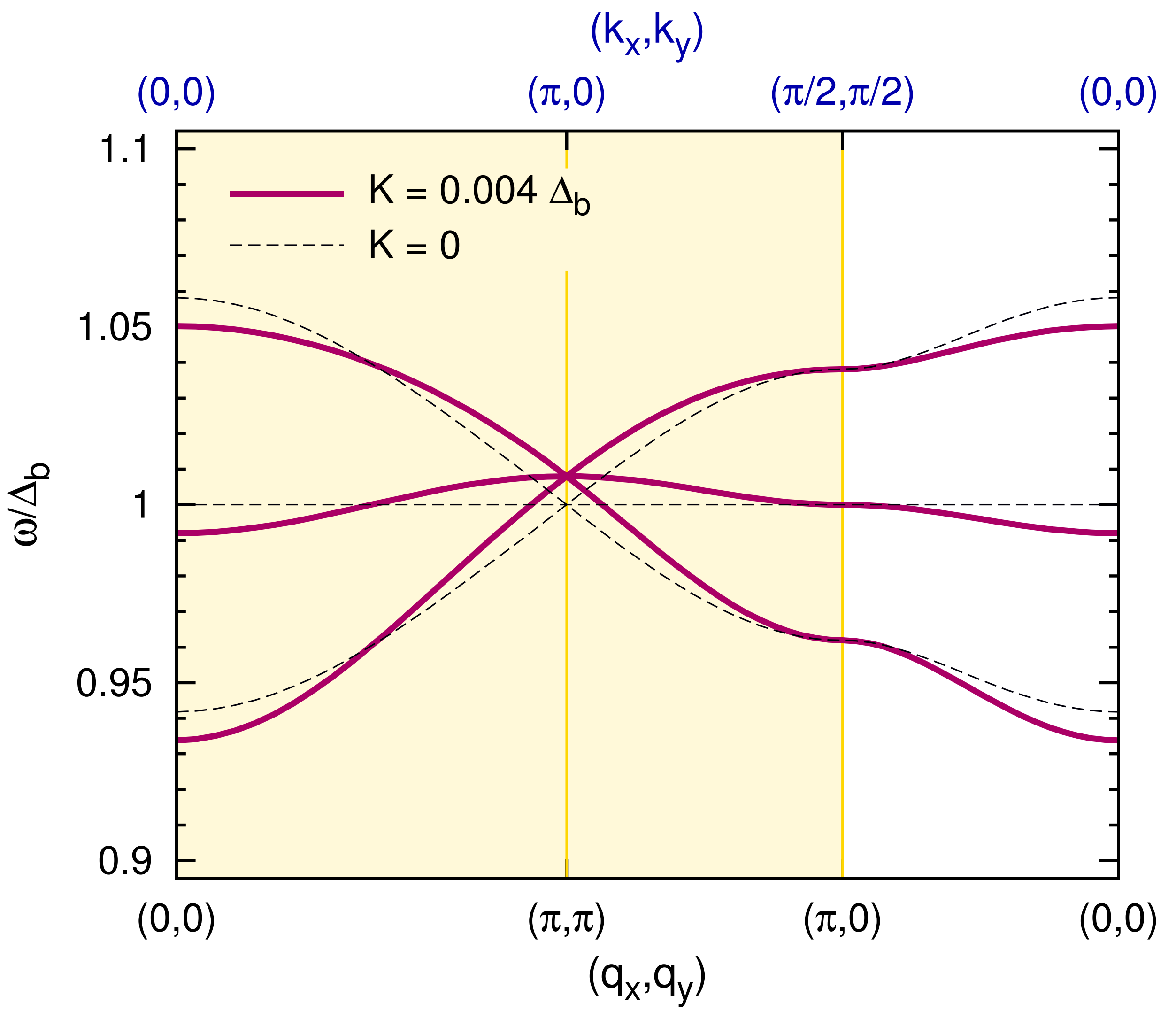

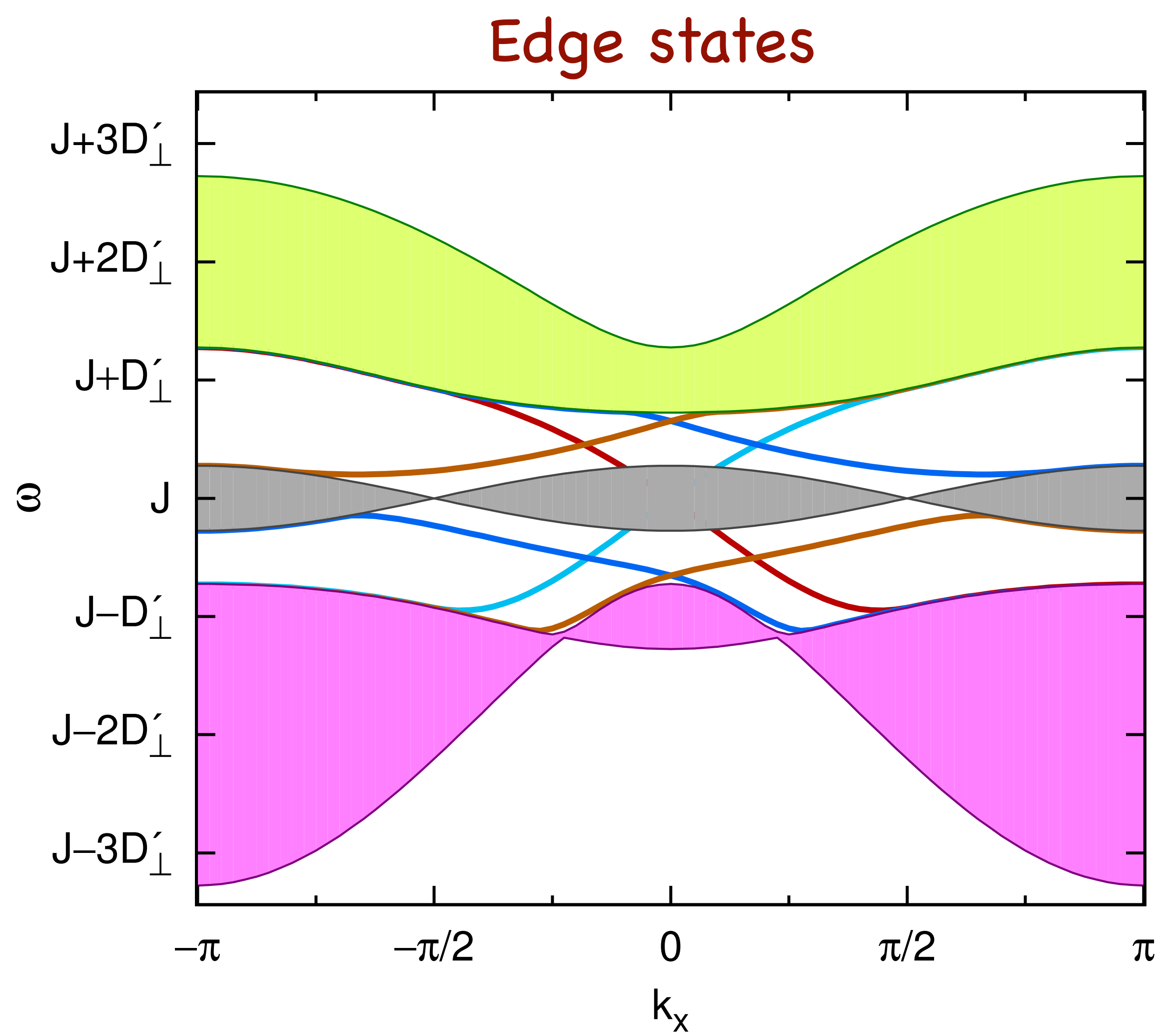

The thermal Hall response

$$\kappa^{xy} = \int_{\mathrm{BZ}} d^2\mathbf{k} \frac{(\omega_0(\mathbf{k})\beta)^2}{2\sinh^2(\frac{\omega_0(\mathbf{k})\beta}{2})} \frac{\mathbf{d}}{d^2} \cdot \left(\frac{\partial \mathbf{d}}{\partial k_y} \times \frac{\partial \mathbf{d}}{\partial k_x} \right).$$

does not change for small K hopping,
as the wave functions unaffected

$$\mathcal{H}(\mathbf{k}) = [J - K_2\gamma_4(\mathbf{k})] + \mathbf{d}(\mathbf{k}) \cdot \mathbf{Q}$$

Summary

- DM interactions lead to Dirac cone in the excitation spectrum
- Chern numbers ± 2 → topological triplon bands
- Protected edge states
- Observable thermal Hall signature
- Topological effects in plateaux phases of $SrCu_2(BO_3)_2$ or other dimer/paramagnetic systems ?
- How to apply general symmetry arguments?
- **Look for the level crossings in the ESR spectra !**

Thank you for your attention